IEEE Access
Multidisciplinary | Rapid Review | Open Access Journal

Received March 14, 2022, accepted April 18, 2022, date of publication April 22, 2022, date of current version May 5, 2022.

Digital Object Identifier 10.1109/ACCESS.2022.3169749

Improved Squirrel Search Algorithm Driven Cascaded 2DOF-PID-FOI Controller for Load Frequency Control of Renewable Energy Based Hybrid Power System

GEETANJALI DEI[1], DEEPAK KUMAR GUPTA[1], BINOD KUMAR SAHU[2], (Member, IEEE), AMITKUMAR V. JHA[1], BHARGAV APPASANI[1], HOSSAM M. ZAWBAA[3,4], AND SALAH KAMEL[5]

[1]School of Electrical Engineering, Kalinga Institute of Industrial Technology (Deemed to be University), Bhubaneswar 751024, India
[2]Department of Electrical Engineering, Siksha 'O' Anusandhan (Deemed to be University), Bhubaneswar 751030, India
[3]Faculty of Computers and Artificial Intelligence, Beni-Suef University, Beni Suef 62511, Egypt
[4]CeADAR Irelands Center for Applied AI, Technological University Dublin, Dublin, D7 EWV4 Ireland
[5]Electrical Engineering Department, Faculty of Engineering, Aswan University, Aswan 81542, Egypt

Corresponding author: Hossam M. Zawbaa (hossam.zawbaa@gmail.com)

The work of Hossam M. Zawbaa was supported by the European Union's Horizon 2020 Research and Enterprise Ireland through the Marie Skłodowska-Curie under Grant 847402.

ABSTRACT Renewable energy-based hybrid power systems are being increasingly deployed across the globe to reduce carbon emissions. The system frequency and tie-line power tend to fluctuate due to system operating conditions. These fluctuations can be maintained within the desired limits using optimally designed controllers. In this article, the recently developed improved squirrel search algorithm (ISSA) is used to tune the parameters of different controllers, such as the proportional-integral-differential (PID), two degrees of freedom PID (2DOF-PID), three degrees of freedom PID (3DOF-PID), and a cascaded 2DOF-PID fractional order integral (FOI) to improve the performance of the system. The effectiveness of the best controller tuned with ISSA is compared with other optimization techniques such as Particle Swarm Optimization (PSO) and Squirrel Search Algorithm (SSA). A two-area multi-machine hybrid power system is considered to demonstrate the robustness of the proposed concept. The first area consists of a thermal, a hydro, and a wind power plant, while the second area consists of a thermal, a hydro, and a diesel power plant. Comparative performance analysis is carried out to obtain the best controller, tuned with the best optimization technique. Various case studies have been developed to check the system's robustness, flexibility, and reliability.

INDEX TERMS Improved squirrel search algorithm (ISSA), integral time multiplied by absolute error (ITAE), load frequency control (LFC), particle swarm optimization (PSO), PID, squirrel search algorithm (SSA).

I. INTRODUCTION

Renewable energy is being explored to minimize the carbon emissions of traditional sources. Consequently, modern power systems consist of both renewable and non-renewable energy sources. A multi-area power system having multiple generators operates at the rated frequency and voltage. If there is an imbalance between the generated power (P_g) and the instantaneous load (P_d), the base frequency deviates from the rated value [1]. If Pg is less than Pd, the generators' speed decreases, consequently decreasing the system's frequency and vice versa. The main requirement of a multi-area power system is the stable frequency of operation as unstable frequency deteriorates its power quality. Automatic gain control (AGC) is used to attenuate the frequency fluctuations and maintain the power quality. The increasing size of the power system and the increasing power demand make the AGC's task of maintaining frequency stability

The associate editor coordinating the review of this manuscript and approving it for publication was Zhenzhou Tang.

challenging [2]. Installation of an adequate controller is very important to reduce the frequency and tie-line power variation under different operational shifts.

A. LITERATURE SURVEY

Several AGC techniques have been proposed to maintain the frequency stability of the power system, such as optimal control techniques, fuzzy logic-based control techniques, adaptive neuro-fuzzy inference system-based control techniques, etc. Genetic algorithm (GA), particle swarm optimization (PSO), differential evolution (DE), teaching learning-based optimization (TLBO), etc., have been used to optimize the parameters of the controller and to improve the dynamic responses of the system. Among various optimization techniques, Genetic Algorithm (GA) has been implemented and reported in [3] for load frequency control under three area test systems in deregulated environment. Nanda *et al.* employed an integral (I) controller in a hydro-thermal system, with constraints on the generate rate in continuous and discrete modes with the help of Bacterial Foraging-Based Optimization Technique [4]. Golpira *et al.* implemented the GA technique in a three-area system to investigate the effects of time delay, Governor Dead Band (GDB) and Generation Rate Constraint(GRC) [5]. Hybrid bacteria foraging optimization algorithm with PSO has been reported to deal with the issue of a load frequency control for linear and nonlinear interconnected systems [6]. Rabindra Kumar *et al.* considered the non-linearity of the governor dead band for maintaining frequency using DE optimized parallel 2-DOF PID controller [7]. Sahu *et al.* proved the supremacy of fuzzy-PID controller based on hybrid DEPSO with a conventional PID controller [8]. Nanda *et al.* considered a three-area thermal power system and used the minority charge carrier-inspired algorithm for implementing the AGC [9]. Dash P. *et al.* implemented a PI-PD cascade controller in a multi-area power system and explained the controller's performance by tuning its parameter by integrating the flower pollination algorithm [10]. Sahu *et al.* proposed a 2-Degree of Freedom Proportional–Integral–Derivative controller based on the TLBO algorithm [11]. Saha *et al.* designed a controller by cascading two degrees of freedom proportional-integral-derivative with a filter (2DOF-PIDN) and a fractional-order integrator controller [(2DOF-PIDN)-FOI] [12]. The whale optimization algorithm (WOA) is implemented to optimize the controller gains of PIDN, PIDN-FOI, and (2DOF-PIDN)-FOI controller. The system analyzed by the author was integrated with electric vehicles, distributed generation, and energy storage devices. Gupta *et al.* reported comparing different optimization techniques such as GSA, FA, and PSO to apply load frequency control in a hybrid power system [13]. Hassanein Hany M *et al.* investigated the time response of a power system by incorporating renewable sources and tuning the parameters using the whale optimization algorithm [14]. Abd-Elazim *et al.* developed a controller for implementing FA in a hybrid system consisting of a thermal generator and photovoltaic (PV) system [15]. The developed controller's response is much better than the GA optimized controller. Jha *et al.* incorporated several optimization techniques, such as the GA, PSO, and firefly algorithm (FA), to optimize the parameters of PI controllers in a hydro-thermal system [16]. Cao *et al.* investigated the system's performance using PSO by designing a fractional order controller [17]. A detailed guide to multi-objective optimization techniques for meta-heuristics application is reported. In this paper, a multi-source system incorporating hydro and gas units was tested to verify the effects of GRC and GDB. The system was analyzed with and without RFB. Mohapatra *et al.* analyzed a system implementing a quasi-oppositional-based salp swarm algorithm to tune the controller gains [18]. A new hybrid gravitational search algorithm with firefly has been used to tune the PID controllers for the LFC of two area systems [19]. An improved PSO has been reported for applying LFC for two area hybrid test systems [20]. Wang *et al.* reported event-based secure H∞ load frequency control for a delayed power system under different operational shifts [21]. Saikia *et al.* implemented integral controllers based on Bacteria foraging optimization to investigate a hydro-thermal system with three unequal areas [22].

Along with different intelligent optimization techniques for tuning parameters of controllers for LFC, an artificial neural network (ANN) has been implemented for various controllers for improving the performance of the multi-area hybrid system. Padhy *et al.* demonstrated the supremacy of hybrid stochastic fractal search and pattern search optimization algorithm over TLBO and DE for the single area and multi-area multi-source power systems incorporating PEV [23]. Arya *et al.* presented an imperialist competitive algorithm (ICA)-based FPIDN-FOI controller, which outperforms under various system parameters and various load demands considering different non-linearities in restructured scenarios [24]. The supremacy of the controller is verified by comparing it with PID/PIDN/FPIDN controllers. Integrated layered recurrent ANN has been reported as a robust control strategy for various operating conditions for handling load frequency control problems [25]. Nayak *et al.* incorporated a two degree of freedom - PID controller optimized by DE algorithm presenting GRC, GDB, and reheat type turbine [26]. Fuzzy logic-based controller has been reported for frequency stabilization under a deregulated environment [27].

Apart from various intelligent optimization techniques used to maintain the frequency variation and tie-line power to minimum values, various researchers have used different controllers for multi-area multi-machine systems. Monje *et al.* designed an FO-PID controller to fulfil the design specifications and get the system's robust performance for variation in controller gain [28]. Hamamci *et al.* analyzed the stability of the fractional-order PID (FOPID) controller and fractional-order PI (FOPI) controller. Hamamci demonstrated the better performance of the FOPID controller and FOPI controller in comparison to the classical controller [29]. J. nanda reported a novel controller for frequency stabilization for hybrid thermal, hydroelectric systems in [30].

Vilanova *et al.* addressed the robustness of the Two-Degree-of-Freedom PI controller by implementing simple tuning rules [31]. Kim *et al.* suggested a 3-DOF-EI-PID controller with emotion function [32]. The immune algorithm optimizes the controller. Debbarma at. al. reported a non-integer controller for LFC of multi-area thermal systems under deregulated environment [33]. Arya *et al.* demonstrated the dynamic behavior of power systems incorporating gas, hydro, and thermal plants by implementing Fractional Order Fuzzy (FOF)-PID controller and using redox flow batteries [34]. Nayak *et al.* designed an interval type-2 fuzzy-PID controller with a derivative filter and analyzed the system time response by implementing the Adaptive-SOS optimization [35]. Sasmita Padhy used a cascaded PI-PD controller tuned with hybrid stochastic fractal search and pattern search technique for AGC of multi-source power systems in the presence of plug-in electric vehicles [23]. (1+ PD)-PID cascade controller for the better performance of the system under diverse power systems has been reported in [36]. The design of cascade-IλDμN controller is reported to deal with the issue of LFC with renewable energy sources and multi-area interconnected thermal and thermal-hydro-gas power systems [37], [38]. Abraham *et al.* implemented superconducting magnetic energy storage in hydro-thermal systems [39]. Bhatti *et al.* presented a power system with parallel AC/DC transmission links. The eigenvalue study concluded that the time response is much better-considering parallel AC/DC links [40]. Saha *et al.* proposed a WOA optimized PIDN-FOPD controller incorporating ultra-capacitor in a multi-area system and a restructured environment [41]. The effect of ultra-capacitor using PIDN-FOPD controller has been investigated for different scenarios like bilateral and contract violation.

B. RESEARCH GAP AND MOTIVATION

Although much research has been reported in designing and simulating the load frequency control in multi-area systems, most of the reported work takes too much time to settle the variation of frequency and tie-line power and excessive effort. Also, the heuristic approach for tuning parameters of various controllers lacks reliability due to not tracking global minima. Furthermore, adequate controller design is required to deal with the issue of LFC and search for the best controller. Hence, many researchers reported the tuning of different controller parameters such as PI, PD, PID, FOPID, and fuzzy-based controllers. The authors used the recently developed 2-degree of freedom PID-FOI controller for maintaining the frequency and tie-line power deviation within the desired values with a fast settling time. A new hybrid evolutionary algorithm called the improved SSA optimization (ISSA) technique was proposed by H. Hu *et al.* in [42], [43], which is yet to be explored for the AGC problem. The work reported in this paper gives the concept of 2DOF-PID-FOI based load frequency control optimized using the recently developed Improved Squirrel Search Algorithm (ISSA) and installed in multi-area multi-machine power systems including renewable energy sources.

C. CONTRIBUTION AND PAPER ORGANIZATION

The main contributions of the proposed work are:

- It is the first to propose the concept for dealing with the issue of LFC by incorporating the use of Improved Squirrel Search (ISSA) for tuning of 2DOF-PID-FOI controllers parameters installed in two areas multi-machine power system.
- A two-area system with different power units is modeled using MATLAB/ Simulink environment.
- Each area consists of three different sources, including non-renewable and renewable units.
- To improve the dynamic response of the considered system, 2-DOF-PID-FOI cascaded controller is implemented.
- A new ISSA optimization technique is applied for the first time in AGC.
- The response of the 2-DOF-PID-FOI cascaded controller is compared with the performance of the PID, 2-DOF-PID, 3-DOF-PID controller to prove its superiority.
- To demonstrate the effectiveness of the proposed concept, different operational shifts (load change) have been considered in the system.
- This work is extended to prove the supremacy of the applied optimization technique by comparing the results with the results of other optimization algorithms like the SSA and the PSO.

D. ORGANIZATION OF THE PAPER

The paper is arranged in five sections. Section 2 describes the ISSA. The linearized models of the two areas multi-unit system and the mathematical formulation adopted to design the controllers are described in the third section. The novel ISSA optimization technique is implemented for the LFC of the test system in section 4 and the results are discussed. The conclusion is discussed in the last section.

II. IMPROVED SQUIRREL SEARCH ALGORITHM

Mohit Jain reported a squirrel search algorithm in 2019 [43]. Hongping Hu proposed a hybrid algorithm combining the squirrel search algorithm and invasive weed optimization (IWO). The reproduction technique in IWO has been added to the normal Squirrel search algorithm to improve the performance of a hybrid algorithm called ISSA [42]. A detailed flow chart of the ISSA is given in fig.1.

The various steps involved in the squirrel search algorithm are described below.

1) GENERATION OF NEW LOCATIONS

Three situations are considered for the dynamic foraging of flying squirrels in the forest without predators. Predators alert the squirrel, compelling it to move randomly over small

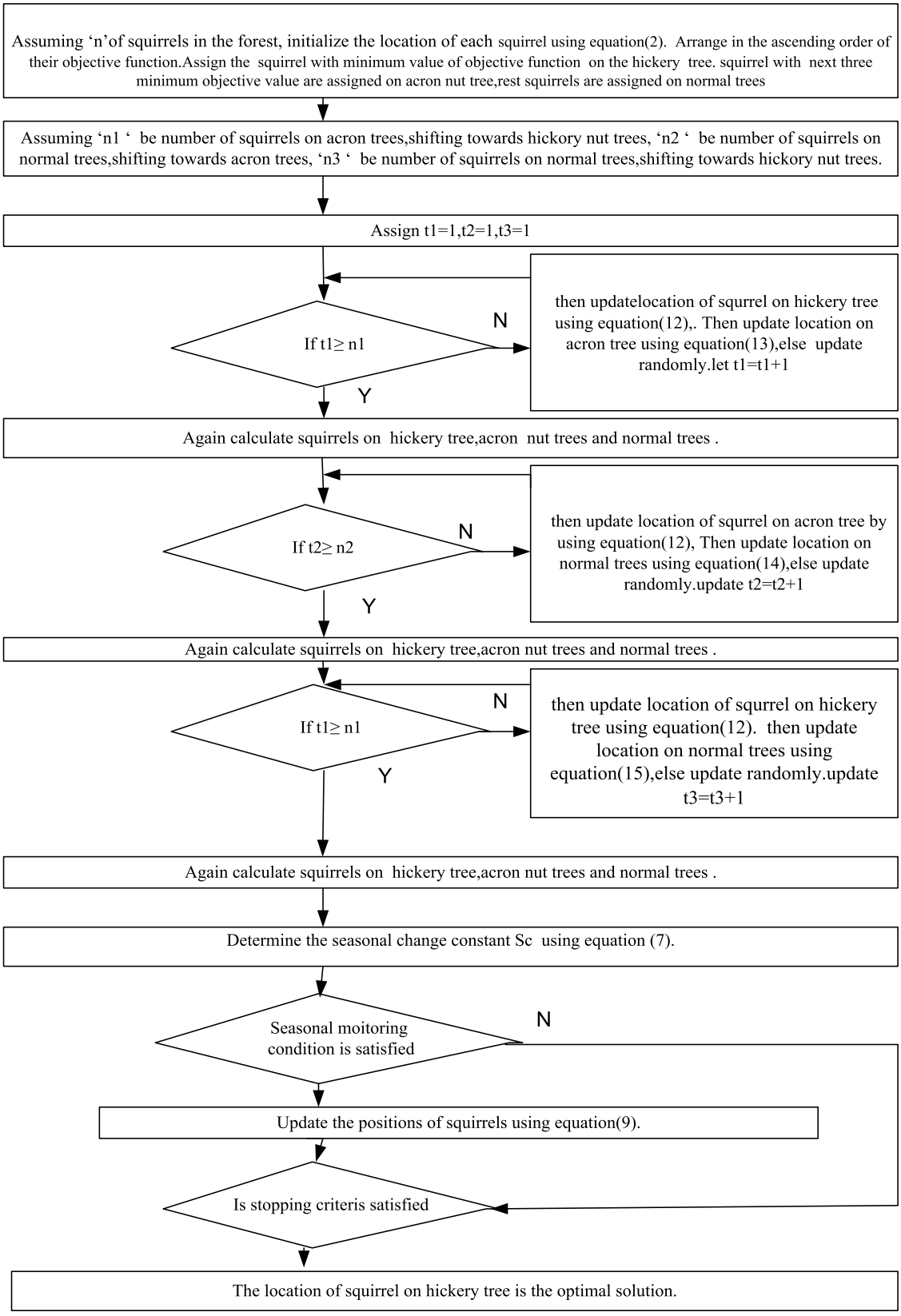

FIGURE 1. Flowchart of ISSA technique for optimal tuning of different controller parameters.

distances, searching for food in a nearby location. T he probability of predator's presence is denoted by P_{dp} and the distances glided by the squirrel is given by d_g.

R_1, R_2, and R_3 are random numbers in the range [0, 1], FS_{ht} is the location of flying squirrel on the hickory tree. The location of squirrels on the acorn nut trees that are adjacent to the hickory nut tree is FS_{at}. The location of the flying squirrels present on the normal trees and cruising towards acorn trees to satisfy their food requirement is FS_{nt}. The current iteration is denoted by t and G_c is the gliding constant. Three different mathematical models describe this dynamic sliding behaviour.

2) INITIALIZATION OF POPULATION

The number of flying squirrels (FS) in the forest is N. The presence of the i^{th} flying squirrel on the i^{th} tree is described by a vector given by the equation (1).

$$FS_i = (FS_{i1}, FS_{i2}, \cdots, FS_{id}), \quad (i = 1, 2, \cdots, N) \tag{1}$$

where FS_{ij} represents the j^{th} dimension of the i^{th} flying squirrel. The initial position of each squirrel is expressed as equation (2).

$$FS_i = FS_L + U\,(0, 1) \times (FS_U - FS_L) \tag{2}$$

where, FS_L and FS_U are lower limit and upper limit on the of i^{th} squirrel's j^{th} dimension respectively and U (0, 1) is an evenly assigned random number in the range [0,1].

3) CLASSIFICATION OF THE POPULATION

Assuming 'N ' no of trees in the forest. There is only one hickory tree in the forest. The number of acorn trees is N_{fs} ($1 < N_{fs} < N$) and the rest are normal trees without food. The total number of squirrels is N.

Depending on the fitness values of the squirrels, squirrels are classified into three categories known as squirrels on hickory trees (Fh), squirrels on acorn trees (Fa), and squirrels located on normal trees (Fn). The squirrels on hickory trees have the lowest fitness value. Depending on the requirement for better food, the desired location is the hickory tree or the acorn tree. The target locations of the squirrels on the normal trees are randomly decided as either the hickory tree or the acorn tree.

4) UPDATING THE LOCATION OF SQUIRRELS

Considering a random number R between 0 and 1, the probability of the predator appearing is denoted by P_{dp}. P_{dp} is assumed as 0.1. If $R > P_{dp}$, the predator is not present, the squirrels are free to search for food in the forest. If $R \leq P_{dp}$, the squirrels are bound to limit their search for food due to predator presence, and they change their locations randomly.

The current iteration is denoted as t; the value of G_c is 1.9; $F_{ai}(i = 1, 2, \ldots\ldots..N_{fs})$ is the population obtained randomly from F_a; d_g can be determined from equation (3):

$$d_g = \frac{h_g}{\tan(\phi) sf} \tag{3}$$

where h_g is taken as 8; the value of sf is 18; the gliding angle $\tan(\phi)$ can be determined using the equation (5):

$$\tan(\Phi) = \frac{D}{L} \tag{4}$$

Applying equation (6) and equation (7), the value of D and L can be calculated using the following equations:

$$D = \frac{1}{2\rho V^2 S C_D} \tag{5}$$

$$L = \frac{1}{2\rho V^2 S C_L} \tag{6}$$

5) MONITORING OF SEASONAL TRANSFORMATION

After modification of the above steps, the season changes are decided by the equations (7) and (8):

$$S_c^t = \sqrt{\sum_{k=1}^{D} \left(F_{ai,k}^t - F_{h,k}^t\right)^2}, \quad i = 1, 2, \ldots, Nfs \tag{7}$$

$$S_{\min} = \frac{10e^{-6}}{365^{\frac{t*2.5}{T}}} \tag{8}$$

where T is the total number of iterations. If $S_c^t < S_{min}$, winter season becomes summer; else, it is winter. When the season changes to summer, squirrels moving toward F_h remain at the new position, other squirrels that shift towards F_a without facing any predators renew the locations by the equation (9):

$$FS_{inew}^{t+1} = FS_L + Le'') \tag{9}$$

Levy is the random walk model. It can be calculated by using the equation (10):

$$Le'vy(x) = 0.01 \times \frac{ra \times \sigma}{|rb|^{\frac{1}{\beta}}} \tag{10}$$

β is assumed as 1.5; σ can be obtained by equation (11):

$$\sigma = \left(\frac{\Gamma(1+\beta) \times \sin(\pi\beta/2)}{\Gamma\frac{(1+\beta)}{2} \times \beta \times 2^{\frac{(\beta-1)}{2}}}\right)^{\frac{1}{\beta}} \tag{11}$$

where, $\Gamma(x) = (x - 1)!$

In the ISSA algorithm, the reproduction technique of IWO is implemented to produce new offspring. For producing the updated position using σ_{iter} three different scenarios have been used in the ISSA technique. SSA is based on three different scenarios for producing the updated position using σ_{iter}.

A. CASE-1

FS_{at} represents the location of individuals that may progress towards hickory nut trees. If $R_1 \geq P_{dp}$, the offspring of every squirrel on the hickory nut tree is calculated using the equation (12).

$$\sigma iter = \frac{(iter_{\max} - iter)^m}{(iter_{\max})^n} \left[\left(\sigma_{initial} - \sigma_{final}\right) + \sigma_{final}\right] \tag{12}$$

Moreover, the locations of the flying squirrels on the hickory tree are recalculated using equation (13).

$$FS_{at}^{t+1} = FS_{at}^t + \left[dg \times Gc \times \left(FS_{ht}^t - FS_{at}^t\right)\right] \tag{13}$$

If $R_1 < P_{dp}$, the location is updated randomly.

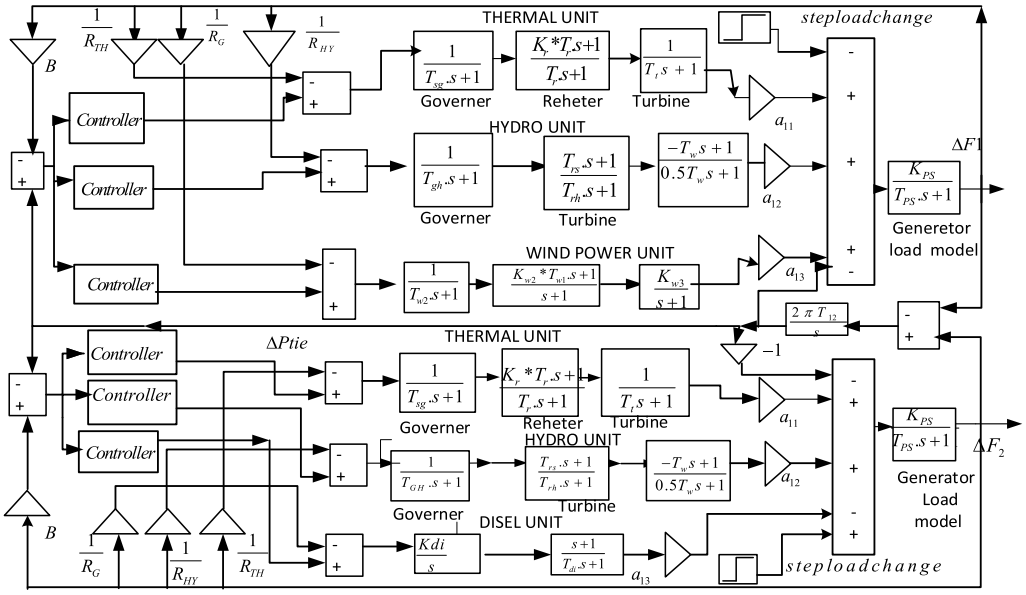

FIGURE 2. Multi area multi machine power system.

B. CASE-2

FS_{nt} represents the location of the individuals proceeding to acorn nut trees for their food. If $R_2 \geq P_{dp}$ the offspring for each of the flying squirrels on the acorn tree is calculated using the equation (12), their positions are recalculated. Equation (14) is used to renew the location of squirrel on the normal trees.

$$FS_{nt}^{T+1} = FS_{nt}^{t} + \left[d_g G_c \left(FS_{at}^{t} - FS_{nt}^{t}\right)\right] \tag{14}$$

If $R_2 < P_{dp}$, the locations are randomly updated.

C. CASE-3

FS_{nt}^{t} represents the location of the individuals that have already consumed the acorn nuts and are going towards the hickory nut tree to store the nuts. If $R_3 \geq P_{dp}$, equation (13) is used to determine the offspring for each individual on the hickory nut tree. The locations of the squirrels on the hickory tree is updated using equation (15).

$$FS_{nt}^{t+1} = FS_{nt}^{t} + \left[d_g \times G_c \times \left(FS_{ht}^{t} - FS_{nt}^{t}\right)\right] \tag{15}$$

If $R_3 < P_{dp}$, the position is updated randomly.

Steps of the ISSA algorithm

1. Initialize population using equation (2).
2. After calculating the fitness of each, the fitness values of all flying squirrels are sorted in increasing order of objective function.
3. Declare the position of flying squirrels on normal trees, acorn trees, and hickory trees.
4. Randomly assume n1 numbers of trees from acron trees gripping towards hickory nut tree & n2 numbers of trees from normal trees gripping towards acorn nut tree and n3 numbers of trees from normal trees shifting towards the hickory tree.
5. Let $t_1 = 1, t_2 = 1, t_3 = 1$
6. If t_1 is more than equal to n1 then again, find the squirrels on normal trees, the acorn trees, and hickory trees; else, go to step-7.
7. If t_1 is less than n_1 perform the Case-I. Update t_1 as $t_1 + 1$. Repeat step-6.
8. If t_2 is more than equal to n_2 then again find the squirrels on acorn trees, the normal trees, and hickory trees; else, go to step-9
9. If t_2 is less than n_2 perform the Case-2. Update t_2 as $t_2 + 1$. Repeat step-8
10. If t_3 is more than equal to n_3 then again, find the individuals on the hickory trees, the acorn trees, and normal trees; else, go to step-11.
11. If t_3 is less, than n_3 perform the Case-3. Update t_3 as $t_3 + 1$. Check whether t_3 is greater than equal to n_1. Repeat step-10.
12. Determine the seasonal constant S_c applying equation (8).
13. Check the Seasonal monitoring condition.
14. If the periodic monitoring condition is fulfilled, then update the position of squirrels in a random manner by implementing the equation (13). Then check the stopping criterion.
15. If the Seasonal monitoring condition is not obtained, check the stopping criterion.
16. If the stopping criterion is not gratified, then go to step-5 and assume $t_1 = 1, t_2 = 1, t_3 = 1$.
17. If the stopping criterion is satisfied, the location of the squirrel on the hickory nut tree is the best location.

III. TEST SYSTEM AND THE PID CONTROLLERS

A. MULTI MACHINE MULTI AREA TEST SYSTEM

Fig. 2 shows the block diagram of the multi-area multi-machine power system. In the given test system, thermal

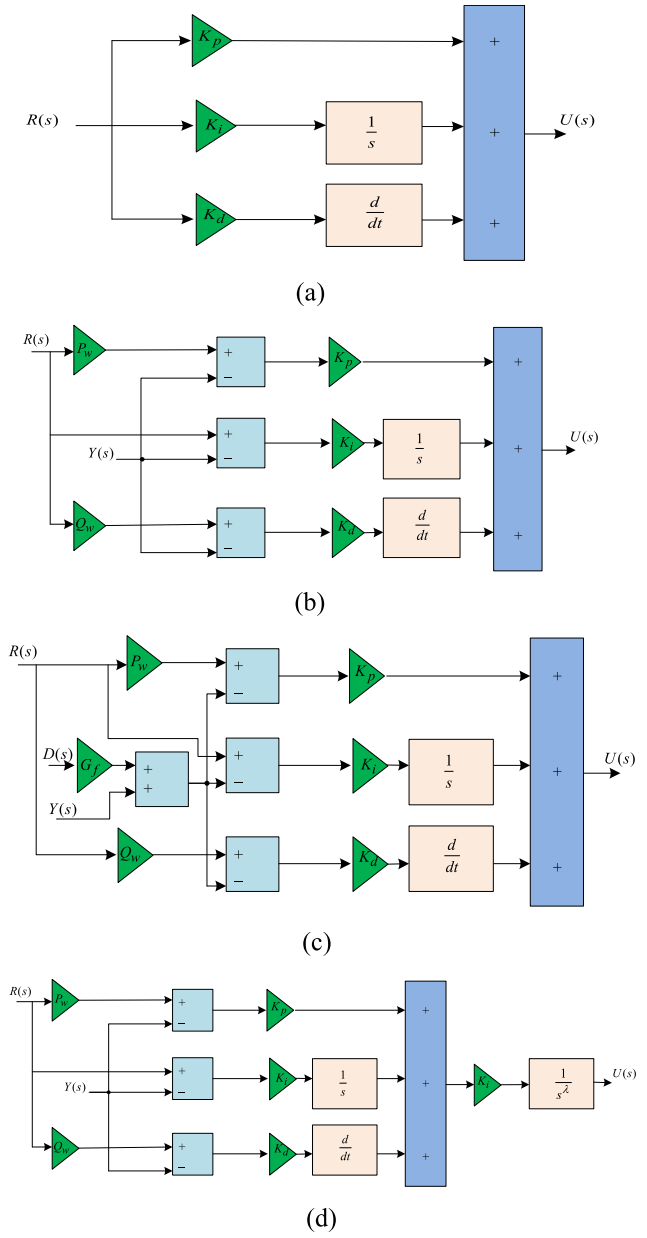

FIGURE 3. (a) Block diagram of PID controller (b) Block diagram of 2-DOF-PID Controller (c) Block diagram of 3-DOF-PID controller (d) 2-DOF- PID-FOI block diagram.

power plant, hydro plant, and wind energy source have been considered in area 1 while Diesel-based power plant and thermal and hydro have been considered in area 2. For every energy source, a controller is used to maintain the frequency and the tie-line power within the desired limit. Various controllers such as PID, 3DOF-PID, 2DOF-PID and 2DOF-PID-FOI have been used to analyze their effectiveness for the LFC under certain operational shifts.

B. PID CONTROLLER

PID controller is a ubiquitous controller which is simple, reliable, and popular. This controller is widely used in industries.

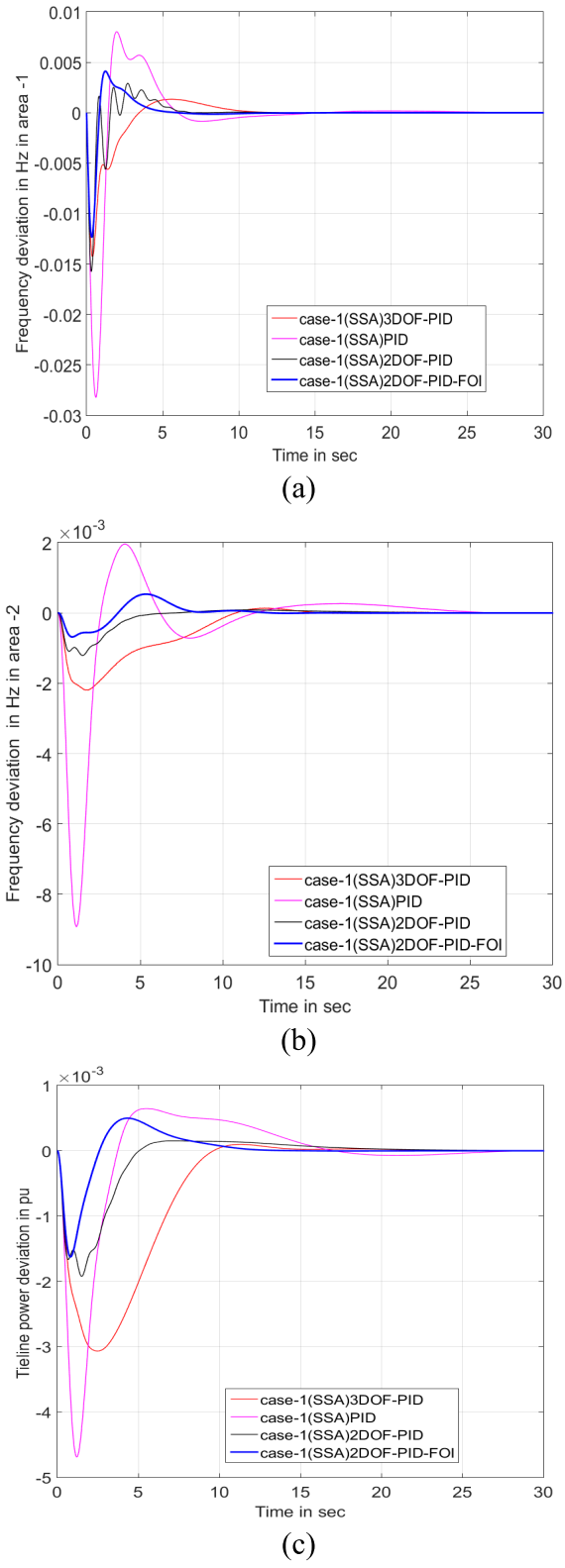

FIGURE 4. Comparison of the dynamic response of the system for SSA based different controllers-Case I. (a) change of frequency in area 1 for SSA based different controller-case-1, (b) change of frequency in area 2 for SSA based different controller -case-1, (c) change of Tie line power for SSA based different controller- case-1.

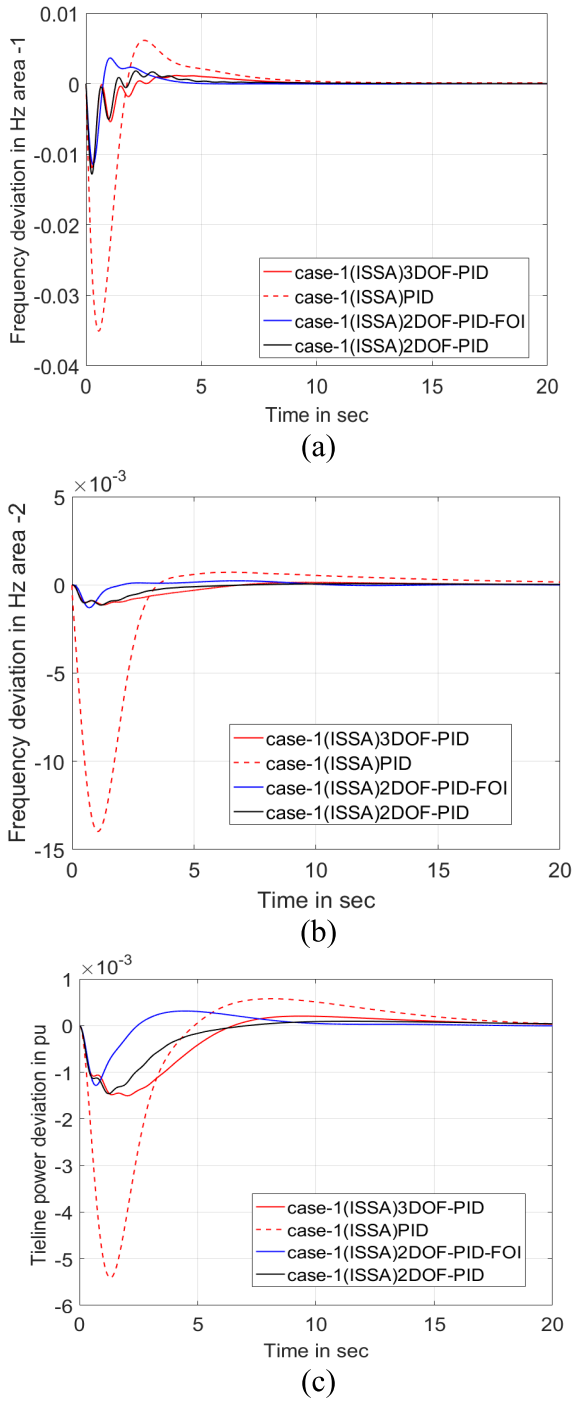

FIGURE 5. Comparison of the dynamic response of the system for ISSA based different controllers-Case I. (a) change of frequency in area 1 for ISSA based different controller-case-1, (b) change of frequency in area 2 for ISSA based different controller -case-1, (c) change of Tie line power for ISSA based different controller- case-1.

It is proved in the literature that the PID controller exhibits superior performance over PI and I controllers. The structure of the PID controller is given by the equation (16).

$$\frac{U(s)}{R(s)} = K_p + \frac{Ki}{s} + K_d s \tag{16}$$

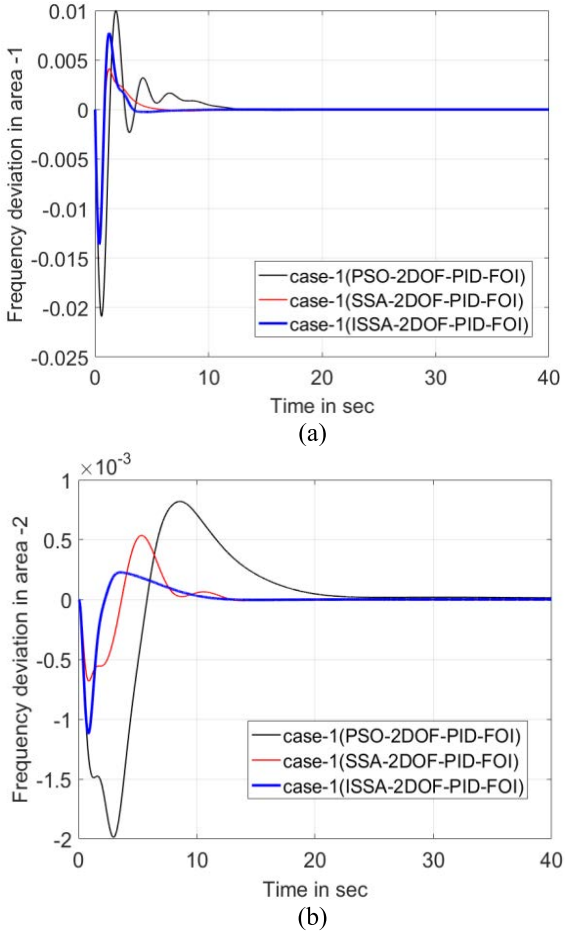

FIGURE 6. Comparison of different optimization techniques for perturbed system response with 2DOF-PID-FOI controllers-Case I. (a) Comparison of different techniques for Δf_1-Case I, (b) Comparison of different techniques for Δf_2-Case I.

C. 2-DOF-PID CONTROLLER

The 2-DOF controller scheme is used by taking certain assumptions on the implementation of the AGC system, such as the feedback noise is assumed to be zero, thereby giving a better control with a faster and more accurate response. Degree of freedom of a control system is the number of closed-loop transfer functions adjusted independently. The design of control systems is a multi-objective problem and, therefore, the two-degree-of-freedom control system can give better response and performance than one-degree of-freedom system. The disturbance is directly applied to the plant system. As per the assumptions, the disturbance that was previously passing through the system and then summed to the output of the plant system is now directly provided as an input to the plant power system. The control scheme is implemented with the PID controller to make the scheme a 2-DOF-PID control scheme. The parameters of this scheme that are to be tuned for efficient control actions are P_W, Q_W, K_P, K_I and $K_{d.}$ Eq (17) represents the output response of the controller.

$$U(s) = \left.\frac{U(s)}{R(s)}\right|_{Y(s)=0} R(s) + \left.\frac{U(s)}{Y(s)}\right|_{R(s)=0} Y(s) \tag{17}$$

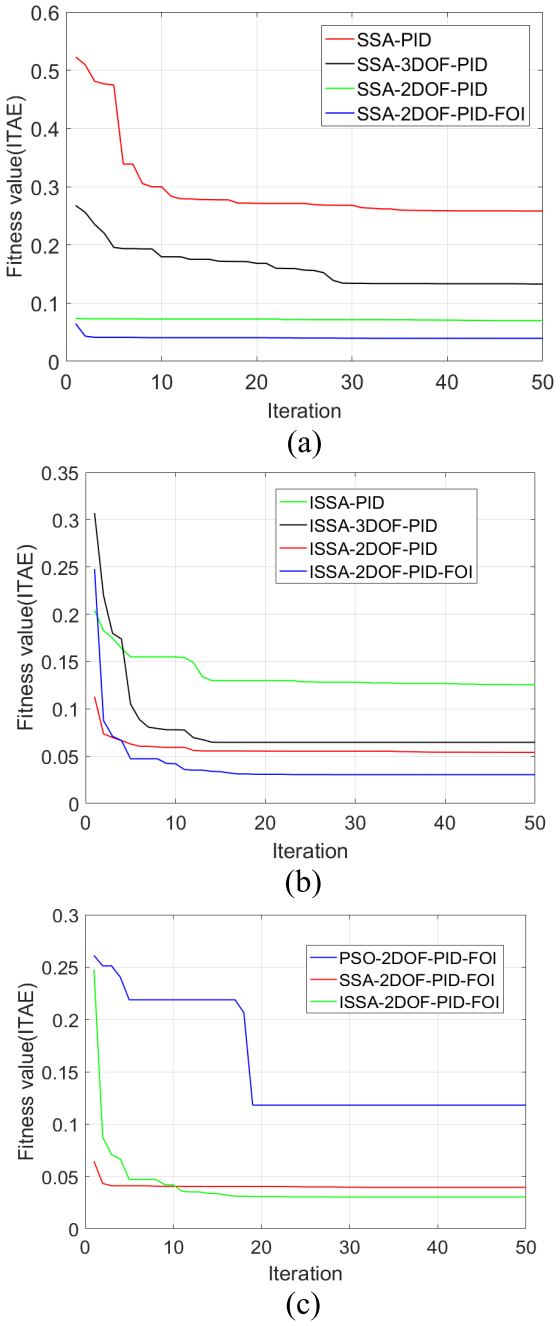

FIGURE 7. Convergence characteristics of SSA, PSO and ISSA with different controllers. (a) Convergence characteristics of SSA with different controller, (b) Convergence characteristics of ISSA with different controller, (c) Convergence characteristics of PSO with different controller.

where

$$\left.\frac{U(s)}{R(s)}\right|_{Y(s)=0} = \left(P_W \times K_P + Q_W \times sK_d + \frac{K_i}{s}\right)$$
$$\left.\frac{U(s)}{Y(s)}\right|_{R(s)=0} = -\left(K_P + sK_d + \frac{K_i}{s}\right)$$

D. 3-DOF-PID

The degree of freedom represents the number of independent control loops that independently perform their control action

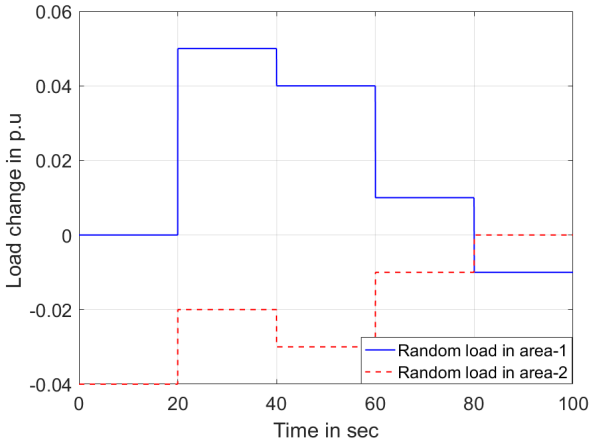

FIGURE 8. Dynamic operational shift (Load change) in the area 1 and area 2.

in the system. It is observed that 2DOF-PID controller consists of two control loops, whereas the 3DOF-PID controller has three control loops. The three loops in the 3DOF-PID controller enhance the stability and response shaping and eliminate the power system disturbances. The respective area control error is the input $R(s)$ to the 3DOF PID controller. $Y(s)$ is the system output indicating the frequency variations of the control area. D(s) represents the disturbance of the system. The additional loop present in the 3DOF-PID controller is responsible for the faster disturbance clearance in the system. It has six parameters to tune. Eq (18) represents the output response of the controller.

$$\begin{aligned} U(s) = &\left.\frac{U(s)}{R(s)}\right|_{\text{Y(s)=0 \& D(s)=0}} \times R(s) \\ &+ \left.\frac{U(s)}{Y(s)}\right|_{\text{R(s)=0 \& D(s)=0}} \times Y(s) \\ &+ \left.\frac{U(s)}{D(s)}\right|_{\text{R(s)=0 \& Y(s)=0}} \times D(s) \end{aligned} \tag{18}$$

where

$$\left.\frac{U(s)}{R(s)}\right|_{\text{Y(s)=0 \& D(s)=0}} = \left(P_W \times K_P + Q_W \times sK_d + \frac{K_i}{s}\right)$$
$$\left.\frac{U(s)}{Y(s)}\right|_{\text{R(s)=0 \& D(s)=0}} = -\left(K_P + sK_d + \frac{K_i}{s}\right)$$
$$\left.\frac{U(s)}{Y(s)}\right|_{\text{R(s)=0 \& D(s)=0}} = -\left(K_P + sK_d + \frac{K_i}{s}\right)$$

E. 2-DOF-PID-FOI

A 2-DOF-PID-FOI has five parameters to optimize. Due to the fractional-order it is more flexible to set the gains and achieve robust performance. It is quite obvious that fractional order PID (FOPID) controller works on the whole plane, whereas its counterpart PID works at defined points. The FOPID controller has five gains i.e. $K_P, K_d, K_i, \mu, \sigma$, in which the first three parameters are integers and the last two parameters are non-integers. Fig. 3 shows the block diagram of all the controllers.

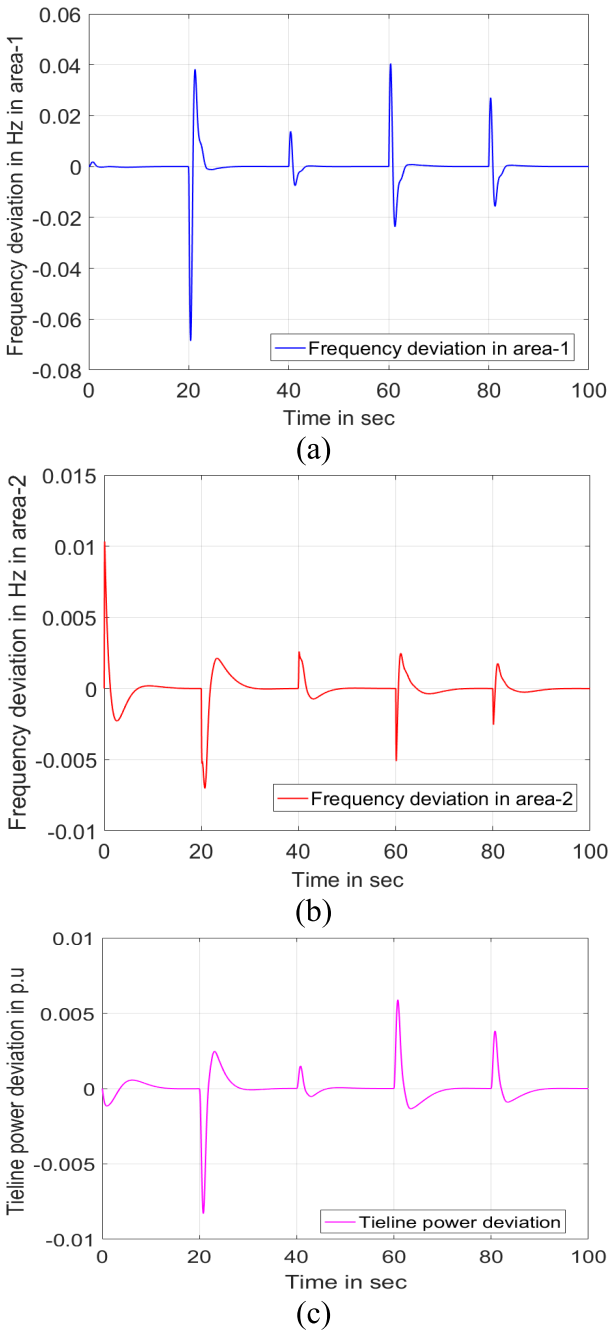

FIGURE 9. Perturbed response of change of frequency in area 1 and 2, and tie-line power variation. (a) change of frequency in area 1, due to random load change, (b) change of frequency in area 2, due to random load change, (c) change of Tie line power due to random load change.

1) FRACTIONAL ORDER INTEGRAL CONTROLLER

The fractional-order integral controller is represented by the equation (19).

$$\frac{U(s)}{R(s)} = \frac{K_I}{s^{\lambda}} \tag{19}$$

2) CASCADE CONTROLLER

Generally, the performance of PID controllers is not satisfactory if the order of the system increases. The presence of non-linearity is another challenge. Cascaded controllers (conglomerating PID and its variants) are introduced to appease the aforesaid problem. This paper has taken an attempt to study the proposed system by cascading PID and FOI controller embedding two degrees of freedom (2-DOF-PID-FOI). Sequential processing of the control signal in a cascaded controller improves the response compared to the normal controller. Equation (20) represents the output response of the controller.

$$\begin{aligned} U_1(s) &= \left.\frac{U_1(s)}{R(s)}\right|_{Y(s)=0} R(s) + \left.\frac{U_1(s)}{Y(s)}\right|_{R(s)=0} Y(s) \\ U(s) &= U_1(s) \times \frac{K_I}{s^{\lambda}} \end{aligned} \tag{20}$$

where

$$\begin{aligned} \left.\frac{U(s)}{R(s)}\right|_{Y(s)=0} &= \left(P_W \times K_P + Q_W \times sK_d + \frac{K_i}{s}\right) \\ \left.\frac{U(s)}{Y(s)}\right|_{R(s)=0} &= \left(K_P + sK_d + \frac{K_i}{s}\right) \end{aligned}$$

IV. RESULTS AND DISCUSSIONS

A three-area power system, each area having three sources, is shown in Fig 2. Four different controllers, namely, PID, 2-DOF-PID, 3-DOF-PID, 2-DOF-PID-FOI, are used to investigate the AGC of the system. Four controllers are employed for the four different sources present in different areas. The controller gains are optimally tuned using the recently developed ISSA algorithm. The SLP (Step Load Perturbation) of 1% is imposed in the first area to examine the frequency stability of the proposed system. A time-domain integral performance index ITAE is chosen to ascertain better control as the objective function considers settling time, overshoot, and undershoot. The fitness function ITAE is expressed in equation (21).

$$J = ITAE = \int_0^{t_{sim}} \left(|\Delta F_1| + |\Delta F_2| + |\Delta P_{tie}|\right) .t.dt \tag{21}$$

In order to determine the optimal controllers' gains, the objective function 'J' is minimized subject to the following constraints:

$$\begin{aligned} &k_{pmin} \le K_p \le k_{pmax}, \quad k_{dmin} \le K_p \le k_{dmax}, \\ &k_{imin} \le K_p \le k_{imax}, \ \sigma_{min} \le \alpha \le \sigma_{max}, \ \mu_{min} \le \mu \le \mu_{max}, \end{aligned}$$

where the maximum and minimum gains of the controller are taken in between 0.01 and 2, and maximum and minimum values.

Various causes have been considered to demonstrate the effectiveness of the ISSA for LFC of multi-area multi-machine power systems. A test system includes a thermal power plant, hydro plant, and wind energy in area 1, while in area 2, the diesel power plant has been used along with thermal and hydro-based energy sources. Comparative performance analysis of different controllers (such as PID,

TABLE 1. Optimally tuned parameters of different controllers with different optimization techniques.

		Kp	Ki	Kd	PW	QW	K_I	Λ	G_f
THERMAL UNITS (Area 1 and Area 2)	ISSA-2DOF-PID-FOI	1.5957	1.9483	1.3509	1.2548	0.3772	2.0000	1.7592	
	SSA-2DOF-PID-FOI	1.9304	2.0000	1.2930	1.3938	0.7777	2.0000	0.3872	
	PSO-2DOF-PID-FOI	0.7588	0.3678	0.3312	1.0875	1.4494	1.1425	0.1208	
	ISSA-2DOF-PID	1.5540	2.0000	1.6190	1.9811	1.0641			
	SSA-2DOF-PID	2.0000	2.0000	0.2949	0.4279	2.0000			
	PSO-2DOF-PID	0.7508	1.6295	1.4638	1.0394	1.1321			
	ISSA-3DOF-PID	0.9379	1.5012	0.6457	1.3111	1.3034			0.0010
	SSA-3DOF-PID	0.0010	0.001	1.6377	2	0.001			2
	PSO-3DOF-PID	0.0100	0.0100	2.0000	0.0100	0.0100			0.0100
	ISSA-PID	2.0000	1.7776	1.9747					
	SSA-PID	0.2056	2.0000	0.4211					
	PSO-PID	1.6193	0.2065	0.9864					
HYDRO UNITS (Area 1 and Area 2)	ISSA-2DOF-PID-FOI	1.8016	0.2687	1.4397	1.8533	0.6873	0.2691	0.9389	
	SSA-2DOF-PID-FOI	0.9688	1.0854	0.7851	0.9410	0.8331	2	0.9454	
	PSO-2DOF-PID-FOI	0.6887	0.3506	0.4982	0.8826	0.2790	1.1378	0.4528	
	ISSA-2DOF-PID	1.4856	1.0278	2.0000	1.0139	0.0100			
	SSA-2DOF-PID	0.3974	0.1174	1.4344	0.7055	0.5161			
	PSO-2DOF-PID	2.0000	0.4900	0.9749	1.2245	1.4074			
	ISSA-3DOF-PID	1.0651	1.4203	1.0478	0.5960	0.7055			0.0097
	SSA-3DOF-PID	0.0010	0.0010	2	2.0000	0.0010			0.0010
	PSO-3DOF-PID	0.0100	2.0000	0.0100	0.0100	0.0100			0.0100
	ISSA-PID	1.9417	0.6261	0.7350					
	SSA-PID	0.7194	0.2023	2.0000					
	PSO-PID	0.3385	0.6940	0.0100					
	ISSA-2DOF- PID-FOI	1.7119	1.6010	0.6110	0.1226	0.7112	1.4208	0.8205	
WIND UNIT (Area 1 Only)	SSA-2DOF- PID-FOI	0.1000	0.1653	1.5761	2	0.2491	0.2243	0.1000	
	PSO-2DOF- PID-FOI	1.3095	0.6963	0.8290	0.3027	1.9819	0.8971	0.5703	
	ISSA-2DOF-PID	2	2	1.0840	1.6594	0.1864			
	SSA-2DOF-PID	0.2773	2	1.9020	2	2			
	PSO-2DOF-PID	1.1733	2.0000	0.1199	0.6780	0.8458			
	ISSA-3DOF-PID	0.6100	1.6940	0.5010	1.1038	0.9938			0.0059
	SSA-3DOF-PID	0.0010	2	2	1.2071	0.0010			0.0010
	PSO-3DOF-PID	2.0000	2.0000	0.0100	2.0000	2.0000			0.0100
	ISSA-PID	0.7929	0.1016	0.8341					
	SSA-PID	0.2120	0.2205	2.0000					
	PSO-PID	0.8764	1.3804	0.8260					
DIESEL UNIT (Area 2 Only)	ISSA-2DOF-PID-FOI	0.9152	0.1000	1.8236	1.7938	0.5683	0.3550	0.8128	
	SSA-2DOF-PID-FOI	1.0240	1.9627	1.0593	0.2965	0.1	0.7912	0.9637	
	PSO-2DOF-PID-FOI	1.3871	0.6639	1.7085	0.9042	0.1417	0.9399	1.5311	
	ISSA-2DOF-PID	0.7471	1.6041	0.0100	1.8337	1.6931			
	SSA-2DOF-PID	1.2690	0.7524	1.1978	0.8542	0.9000			
	PSO-2DOF-PID	1.9688	2.0000	1.4062	0.7297	0.8446			
	ISSA-3DOF-PID	0.6569	2	0.9814	0.9938	1.7488			1.7463
	SSA-3DOF-PID	0.0010	2	2	2	2			0.8666
	PSO-3DOF-PID	2.0000	2.0000	0.0100	0.0100	0.0100			2.0000
	ISSA-PID	1.9650	1.9887	1.4802					
	SSA-PID	0.1015	2	2					
	PSO-PID	0.0100	2	0.0100					

3DOF-PID, 2DOF-PID, and 2DOF-PID-FOI) have been discussed to maintain the frequency variation and the tie-line power flow in LFC. Parameters of these controllers have been optimally tuned by intelligent optimization techniques such as the ISSA, the SSA, and the Particle Swarm Optimization (PSO). ITAE has been considered an objective function. A comparison has been made to obtain the best dynamic behavior of all the state variables for the given test system. The test system of multi-area multi-machine is built in the MATLAB/SIMULINK platform, while the different optimization techniques have been written in MATLAB code (.m file).

A. CASE STUDY I

To analyze the behaviour of different controllers for LFC, 1% load change has been introduced in area 1, and dynamic response for all the state variables is observed. Parameters of all the Controllers (PID, 3DOF-PID, 2DOF-PID, and 2DOF-PID-FOI) have been tuned by three optimization techniques (ISSA, SSA, and PSO) under specific operational shifts. Fig. 4 shows the dynamic behavior change in frequencies of area 1, area 2, and deviation in tie-line power flow for all the four controllers tuned with the Squirrel Search Algorithm (SSA).

TABLE 2. Overshoot/Undershoot and Settling time of state variables for Case I.

		Δf_1			Δf_2			ΔP_{tie}			
Optimization Techniques	**Controller**	$U_{sh}\times10^{-3}$ (Hz)	$O_{sh}\times10^{-3}$ (Hz)	T_s (sec)	$U_{sh}\times10^{-3}$ (Hz)	$O_{sh}\times10^{-3}$ (Hz)	T_s (sec)	$U_{sh}\times10^{-3}$ (Hz)	$O_{sh}\times10^{-3}$ (Hz)	T_s (sec)	ITAE (objective function)
Particle Swarm Optimization (PSO) driven Controllers	2DOF-PID-FOI	-20.6	9.9	11.6	-1.98	0.8	15.27	-4.16	0.77	16.85	0.2953
	2DOF-PID	--15.23	3.96	8.271	-1.447	0.085	5.069	-2.339	0.1	10.18	0.0811
	3DOF-PID	-15.6	3.8	10.93	-1.2	0.1	15.3	-2.4	0.2	15.34	0.1775
	PID	-0024.4	7.41	13.07	-9.4	0.51	14.83	-5.28	0.366	10.03	0.3653
Squirrel Search Algorithm (SSA) driven Controllers	2DOF-PID-FOI	-12.3	4.1	4.745	-0.7	0.5	7.127	-1.6	0.5	7.404	0.05106
	3DOF-PID	-14.3	1.3	10.09	-2.2	0.1	13.19	-3.1	0.1	8.77	0.1702
	2DOF-PID	-15.7	2.9	5.944	-1.2	0.1	11.56	-1.9	0.2	7.586	0.07205
	PID	-28.2	8.0	13.12	-8.9	2.0	20.18	-4.7	0.6	14.01	0.3149
Improved Squirrel Search Algorithm (ISSA) driven Controllers	2DOF-PID-FOI	-13.63	7.735	4.053	-1.109	0.226	4.8473	-01.772	0.4709	5.773	0.0394
	3DOF-PID	--11.94	1.168	8.819	-1.129	0.142	9.465	-1.504	0.2038	10.13	0.1227
	2DOF-PID	-12.86	1.822	6.975	-1.05	0.0625	12.45	-1.462	0.0927	11.63	0.07205
	PID	-17.07	3.757	8.05	-5.303	0.1228	8.887	-3.091	0.3463	13.63	0.1353
Improved Squirrel Search Algorithm (ISSA) driven Controllers (with GRC)	2DOF-PID-FOI	-14.2	9.5	10.61	-1.051	0.2055	11.4	-01.896	0.4177	9.606	0.0396
	3DOF-PID	--7.817	0.962	10.95	-0.9472	0.2113	18.76	-1.33	0.2989	19.56	0.1117
	2DOF-PID	-14.42	3.131	10.02	-1.686	0.087	17.41	-1.935	0.114	19.85	0.0723
	PID	-22.26	3.138	11.08	-6.184	1.143	17.93	-3.703	0.5229	18.46	0.1936

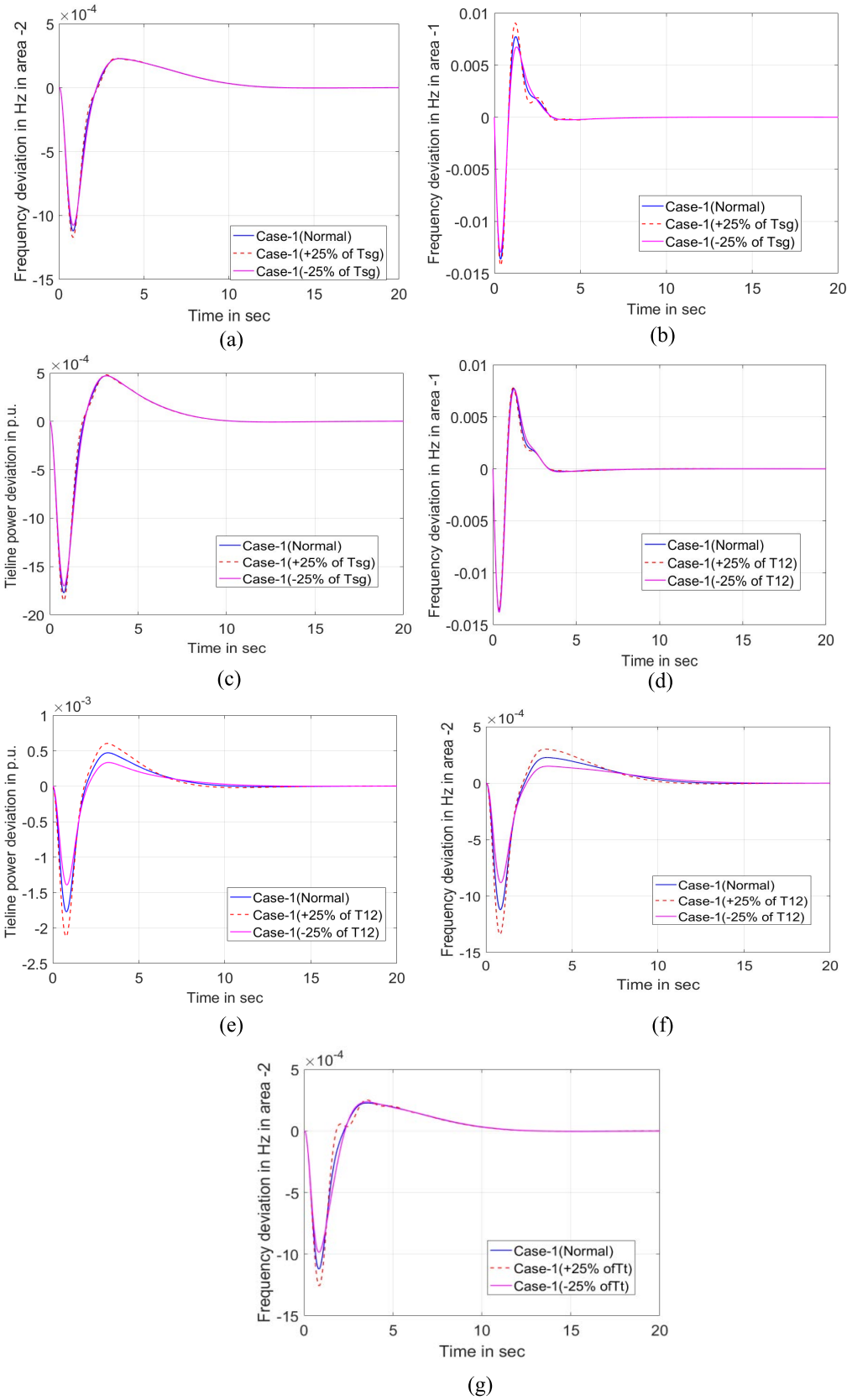

FIGURE 10. Perturbed response of the system with 25 percentage change of system parameters (Tsg, T12 and Tt). (a) Variation of Δf_2 with 25% variation in Tsg, (b) Variation of Δf_1 with 25% variation in Tsg, (c) Variation of $\Delta P_{\text{tie-line}}$ with 25% variation in Tsg, (d) Variation of Δf_1 with 25% variation in T12, (e) Variation of $\Delta P_{\text{tie-line}}$ with 25% variation in T12, (f) Variation of Δf_2 with 25% variation in T12, (g) Variation of Δf_2 with 25% variation in Tt, (h) Variation of $\Delta P_{\text{tie-line}}$ with 25% variation in Tt, (i) Variation of Δf_1 with 25% variation in Tt.

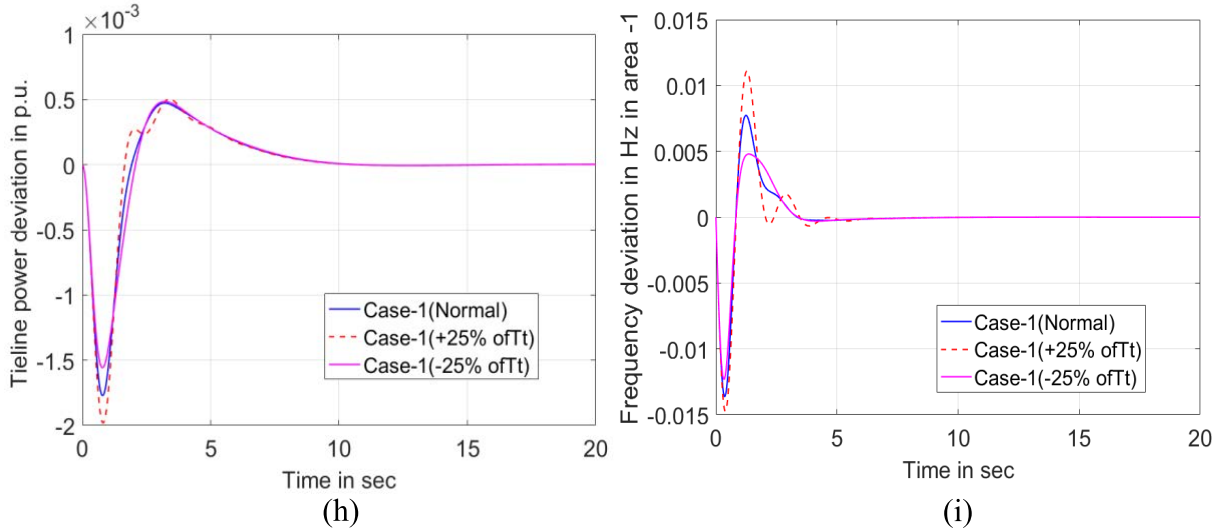

FIGURE 10. *(Continued.)* **Perturbed response of the system with 25 percentage change of system parameters (Tsg, T12 and Tt). (a) Variation of Δf_2 with 25% variation in Tsg, (b) Variation of Δf_1 with 25% variation in Tsg, (c) Variation of $\Delta P_{tie\text{-}line}$ with 25% variation in Tsg, (d) Variation of Δf_1 with 25% variation in T12, (e) Variation of $\Delta P_{tie\text{-}line}$ with 25% variation in T12, (f) Variation of Δf_2 with 25% variation in T12, (g) Variation of Δf_2 with 25% variation in Tt, (h) Variation of $\Delta P_{tie\text{-}line}$ with 25% variation in Tt, (i) Variation of Δf_1 with 25% variation in Tt.**

TABLE 3. **Overshoot/undershoot, settling time under system parameters variation.**

Parameter	Variation In %	Δf_1			Δf_2			ΔP_{tie}			ITAE
		U_{sh} $\times 10^{-3}$ (Hz)	O_{sh} $\times 10^{-3}$ (Hz)	T_s (sec)	U_{sh} $\times 10^{-3}$ (Hz)	O_{sh} $\times 10^{-3}$ (Hz)	T_s (sec)	U_{sh} $\times 10^{-3}$ (Hz)	O_{sh} $\times 10^{-3}$ (Hz)	T_s (sec)	
TsG=0. 08	Normal	-13.63	7.735	4.053	-1.109	0.226	4.8473	-01.772	0.4709	5.773	0.0364
TsG=0.1	+25%	-13.94	9.007	4.053	-1.168	0.226	4.8473	-1.84	0.487	5.773	0.0366
TsG=0.06	-25%	-12.97	6.673	4.053	-1.077	0.226	4.8473	-1.701	0.4703	5.773	0.0364
T12=0.433	Normal	-13.63	7.735	4.053	-1.109	0.226	4.8473	-01.772	0.4709	5.773	0.0364
T12=0.0541	+25%	-13.63	7.735	4.053	-1.34	0.30	5.75	-2.119	0.6032	5.995	0.0378
T12=	-25%	-13.63	7.735	4.053	0.867	0.15	3.993	-1.392	0.334	5.106	0.0353
R	Normal	-13.63	7.735	4.053	-1.109	0.226	4.8473	-01.772	0.4709	5.773	0.0364
R	+25%	-13.67	7.892	4.07	-1.113	0.226	4.794	-1.78	0.4703	5.77	0.0364
R	-25%	-14.2	7.722	3.97	-1.253	0.327	6.2	-1.97	0.643	6.285	0.05
Tw2	Normal	-13.63	7.735	4.053	-1.109	0.226	4.8473	-01.772	0.4709	5.773	0.0364
Tw2	+25%	-13.63	7.735	4.053	-1.109	0.226	4.8473	-01.772	0.4709	5.773	0.0364
Tw2	-25%	-13.63	7.735	4.053	-1.109	0.226	4.8473	-01.772	0.4709	5.773	0.0364
Tw1	Normal	-13.63	7.735	4.053	-1.109	0.226	4.8473	-01.772	0.4709	5.773	0.0364
Tw1	+25%	-13.63	7.735	4.053	-1.098	0.2132	4.8473	-01.737	0.4465	5.773	0.0352
Tw1	-25%	-13.63	7.735	4.053	-1.145	0.241	4.8473	-01.805	0.49	5.773	0.0378

The graph shows that among all four controllers, two degrees of freedom- PID-FOI controller- give the best performance in terms of overshoot/undershoot and settling time. 2DOF-PID-FOI controller outperforms the remaining controllers (such as PID, 3DOF-PID and 2DOF-PID) to give the best system stability and robustness. Similarly, fig. 5 shows dynamic system behavior with improved Squirrel Search Algorithm (ISSA) driven optimum controllers.

From the above graph, it can also be concluded that among all four controllers, two degrees of freedom - PID - FOI- outperform other controllers (PID, 3DOF-PID and 2DOF-PID) in terms of settling time and overshoot/undershoot.

Analysis has been made between three optimization techniques as well (Improved Squirrel Search Algorithm (ISSA), Squirrel Search Algorithm (SSA) and Particle Swarm Optimization (PSO)) to get the best result by optimally

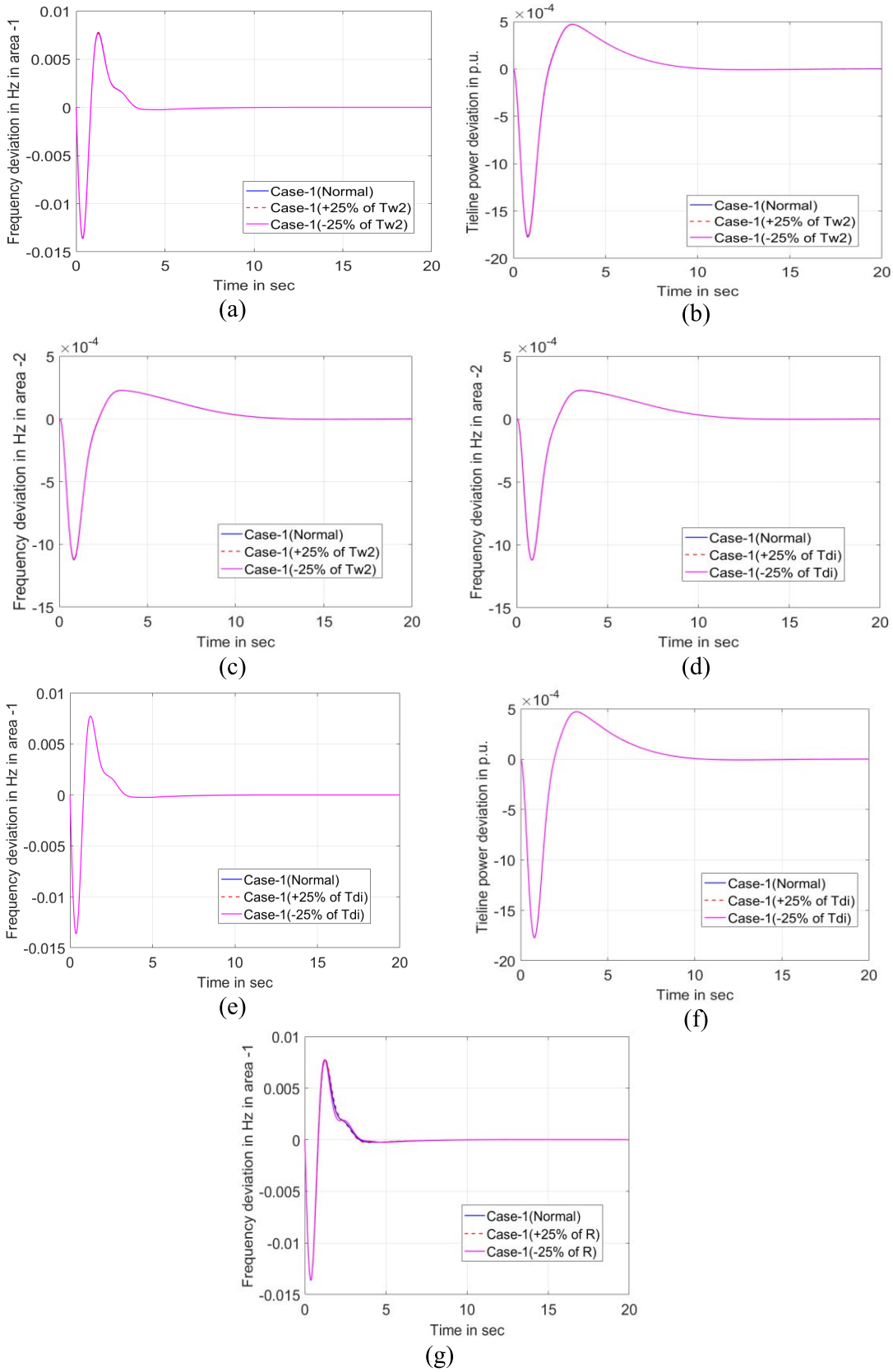

FIGURE 11. Perturbed response of the system with 25 percentage change of system parameters (Tw2, Tdi and R). (a) Variation of Δf_1 with 25% variation in Tw2, (b) Variation of $\Delta P_{\text{tie-line}}$ with 25% variation in Tw2, (c) Variation of Δf_2 with 25% variation in Tw2, (d) Variation of Δf_2 with 25% variation in Tdi, (e) Variation of Δf_1 with 25% variation in Tdi, (f) Variation of $\Delta P_{\text{tie-line}}$ with 25% variation in Tdi, (g) Variation of Δf_1 with 25% variation in R, (h) Variation of Δf_2 with 25% variation in R, (i) Variation of $\Delta P_{\text{tie-line}}$ with 25% variation in R.

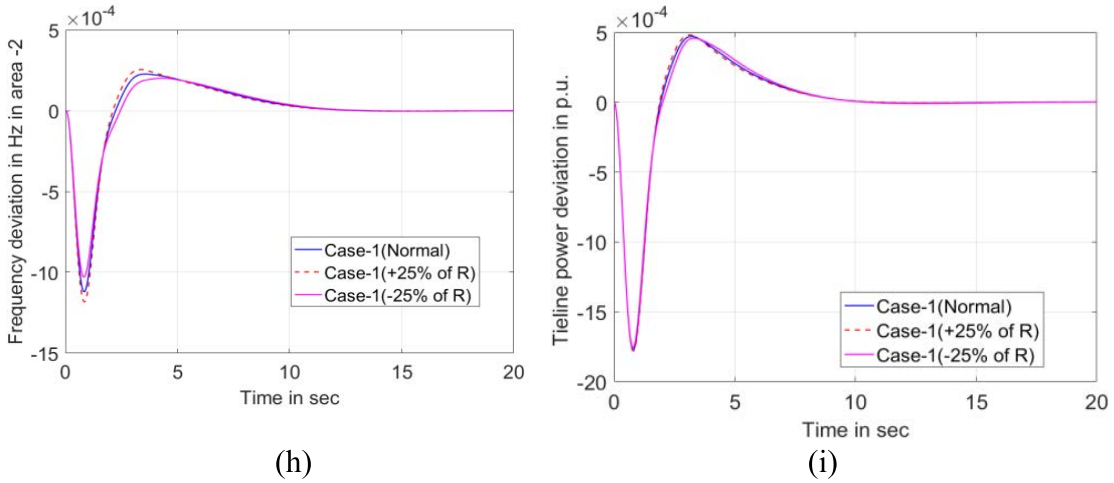

FIGURE 11. *(Continued.)* **Perturbed response of the system with 25 percentage change of system parameters (Tw2, Tdi and R). (a) Variation of Δf_1 with 25% variation in Tw2, (b) Variation of $\Delta P_{\text{tie-line}}$ with 25% variation in Tw2, (c) Variation of Δf_2 with 25% variation in Tw2, (d) Variation of Δf_2 with 25% variation in Tdi, (e) Variation of Δf_1 with 25% variation in Tdi, (f) Variation of $\Delta P_{\text{tie-line}}$ with 25% variation in Tdi, (g) Variation of Δf_1 with 25% variation in R, (h) Variation of Δf_2 with 25% variation in R, (i) Variation of $\Delta P_{\text{tie-line}}$ with 25% variation in R.**

tuning 2DOF-PID-FOI controller's parameters (best controller). Perturbed responses of Δf_1, Δf_{12} and ΔP_{12} are shown in fig. 6 for 2DOF-PID-FOI controller tuned with three optimization techniques by considering 1% load change in area 1 as an operational shift.

Table 1 shows the optimally tuned parameters of different controllers with different optimization techniques. Overshoot/undershoot, settling time for all the states variables, and the final value of an objective function for case 1 (1 percentage load change in area 1) is depicted in Table 2. From the table, it is obvious that the ISSA-based 2ODF-PID-FOI controller significantly improves the system compared to the PSO driven and SSA driven controllers. Performance of 2 degrees of freedom PID FOI controller outperforms other controllers to improve system stability, reliability, and robustness.

To track the best possible values of controller's parameters within the desired values, the performance of all the three optimization techniques has been compared iteration wise in fig. 7. The figure shows that the improved squirrel search algorithm (ISSA) is tracking the best optimal solution in quick time compared with PSO and SSA optimization techniques. The same can be stated for 2DOF-PID-FOI controller as well, which gives the minimum value of the objective function in comparison with other controllers.

B. CASE STUDY II

In this case, an investigation is made on the robustness of the proposed concept of ISSA driven 2DOF-PID-FOI controller for load frequency control with large load changes on a frequent basis. The flexibility of the proposed concept has been addressed by changing load in both areas after 20 seconds each.

Fig. 8 shows the step load change in both areas with respect to time. Random load change in area 1 is represented by the blue line, while the red line represents the load change in area 2. Deviation in the frequency of areas 1 and 2, along with a change in tie-line power, is shown in fig. 9. The system has been simulated with 2DOF-PID-FOI controller tuned with ISSA optimization technique for initial load change. From fig. 8, it can be observed that the proposed concept for dealing with LFC problem gives better system dynamics, reliability and flexibility of the power system for dynamical change in the load at regular intervals.

C. CASE STUDY III

The effectiveness of the proposed concept for load frequency control (LFC) has been verified under the variation of different test system parameters (dynamic operational shifts). Variation of these different parameters such as time constant of speed governor of thermal power plant (Tsg), stiffness coefficient (T12), time constant of the steam turbine (Tt) and hydro power plant (Tw), time constant for diesel power plant (Tdi), and droop governor characteristic (R) have been considered with 25 percent change in their values (both positive and negative). Fig. 10 shows the perturbed response of frequencies for areas 1 and 2 and a tie-line power variation with 25 percentage variations of Tsg, T12, and Tt.

Fig. 11 shows the perturbed response of frequencies for areas 1 and 2 along with the variation of tie-line power with 25 percentage variation of the 'system's Tw2, Tdi, and R parameters. From the figures, it can be depicted that the test system remains stable even with change in the different system parameters. This validates the flexibility and robustness of the proposed concept for dealing with the problem of load frequency control for multi-area multi-machine power systems.

Table 3 gives the values of settling time, overshoot/undershoot of tie-line power and frequencies of areas 1 and 2 for variation of different parameters. All these case

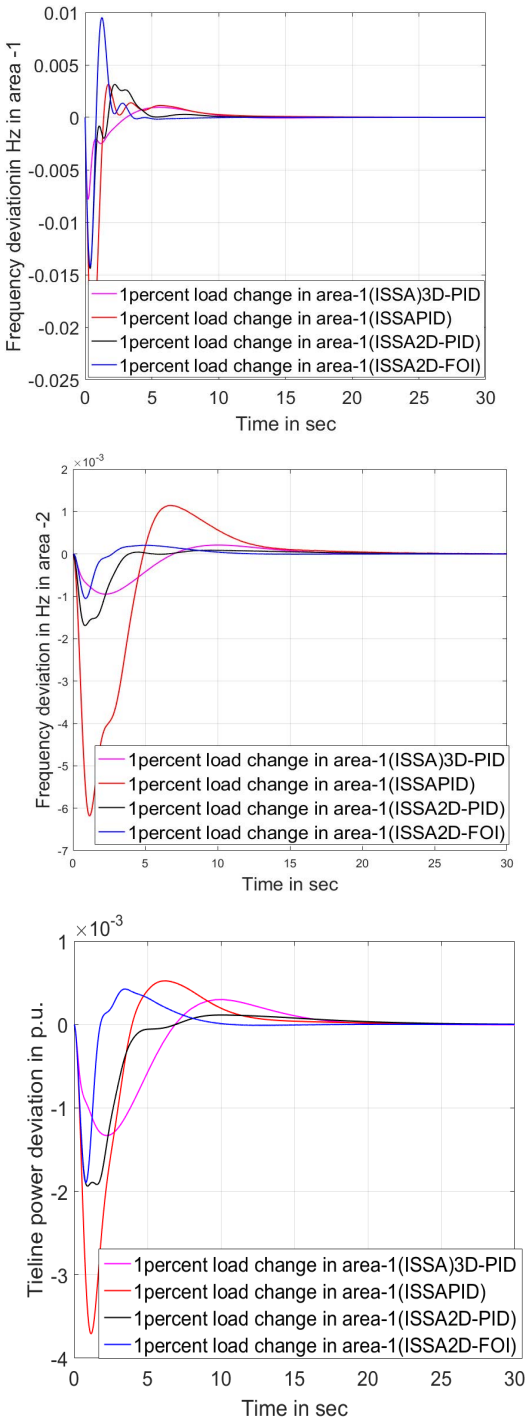

FIGURE 12. Perturbed response of change in frequency and tie-line power with Generation Rate Constraint (GRC).

studies and their result show the proposed concept's effectiveness in tuning 2DOF-PID-FOI controllers parameters with the ISSA optimization technique.

D. CONSIDERING GENERATION RATE CONSTRAINT (GRC) NON-LINEARITY

The demonstrate the robustness of the proposed ISSA driven 2DOF-PID-FOI controller, Generation Rate Constraint

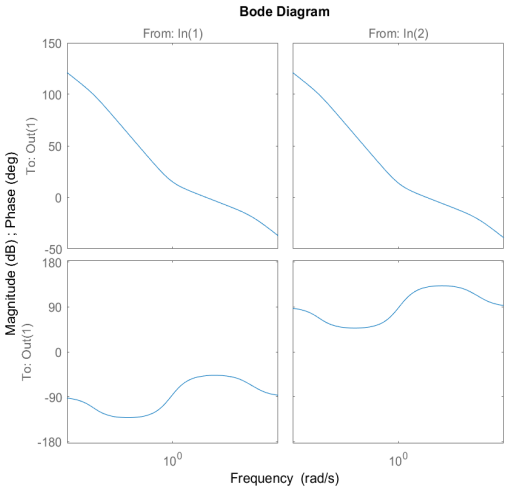

FIGURE 13. Bode plot of the entire system with 2DOF-PID-FOI controller.

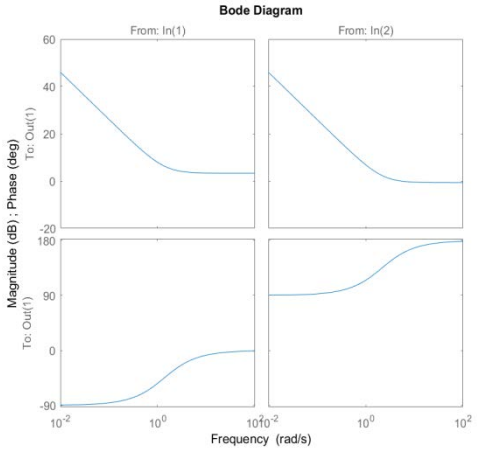

FIGURE 14. Bode plot of the entire system with 2DOF-PID controller.

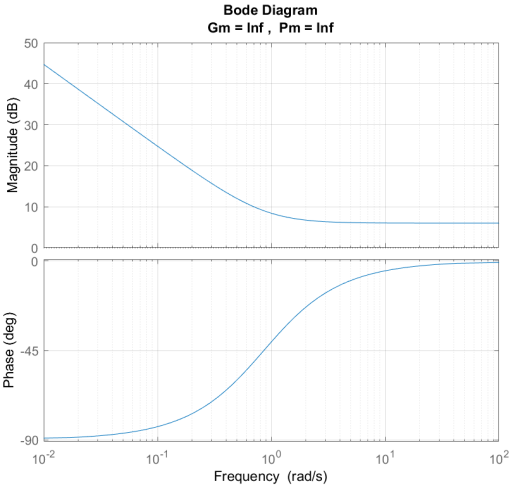

FIGURE 15. Bode plot of the entire system with PID controller.

(GRC) non-linearity is considered. The maximum and minimum limit for the output of the reheat thermal power plant is considered as 10% and for hydro power plant maximum GRC is 350% and minimum limit is 270%. Deviation in frequency and tie-line power exchange is shown in figure 12

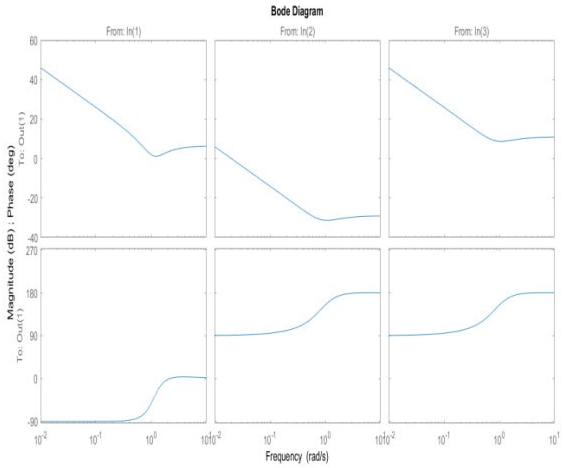

FIGURE 16. Bode plot of the entire system with 3DOF-PID controller.

with the comparison of different controllers tuned with ISSA optimization technique. Table 2 shows the settling time and overshoot/undershoot of the different variables. From the figure and table is can be observed that ISSA driven 2DOF-PID-FOI controller gives better dynamic response under different operational shifts with less settling time and overshoot/undershoot.

E. FREQUENCY DOMAIN STABILITY TEST (BODE PLOT)

To validate the proposed concept of ISSA driven 2DOF-PID-FOI controller for hybrid test system, frequency domain stability analysis has been carried out with bode plot. Figures 13-16 give the bode plot of the system using the proposed 2DOF-PID-FOI controller, along with 2DOF-PID, PID and 3DOF-PID controller, which shows the positive value of gain margin (GM) and phase margin (PM) and hence the stable system.

V. CONCLUSION

This paper proposes the novel concept of ISSA driven 2DOF-PID-FOI controller for maintaining frequency and tie-line power deviation within the desired limit in a hybrid power system under different operational shifts. Optimal tuning of different controller's parameters has been tuned with newly developed ISSA optimization techniques by minimizing ITAE performance indices. A multi-area multi-machine hybrid power system is considered to demonstrate the effectiveness of the proposed concept. Area 1 includes thermal, hydro, and wind power plants, while area 2 includes thermal, hydro, and diesel plants. The effectiveness of the best controller tuned with ISSA is compared with other optimization techniques such as Particle Swarm Optimization (PSO) and Squirrel Search Algorithm (SSA). Comparative performance analysis is carried out to find the best controller tuned with the best optimization techniques. Various case studies have been developed to check the robustness and flexibility along with improved reliability of the hybrid system. From the results, it can be concluded that the 2DOF-PID-FOI controller gives the best transient performance, when tuned with the ISSA optimization technique compared to other controllers. The proposed concept for dealing with the LFC problem is validated under dynamical change of load (random load variation), non-linearities of the system (Generation Rate Constraint (GRC)) and also for different system parameter variations. The proposed concept's effectiveness is analyzed in terms of settling time, overshoot/undershoot of all the system's states variable's transient response.

APPENDIX

$K_{w2} = 1.25$; $K_{w3} = 1.3$; $T_{w1} = 0.6$; $T_{w2} = 0.041$ s; $K_{di} = 16.5$; $T_{di} = 0.025$ s; $K_D = 0.138$; f = 60 Hz; $K_{PS} =$ 68.9566 Hz/ p.u Mw; $T_{PS} = 11.49$ s; $T_{sg} = 0.08$ s; $T_t = 0.3$ s; $T_{12} = 0.0433$ s; $R_{TH} = 2.4$ Hz/ p.u Mw; $R_{HY} = 2.4$ Hz/ p.u Mw,; $R_G = 2.4$ Hz/ p.u Mw,; B = 0.4312; $K_r = 0.3$; $T_r =$ 10.0 s; $T_W = 1$ s; $T_{rs} = 5$ s; $T_{rh} = 28.75$ s; $T_{gh} = 0.2$ s; $a_{11} = 0.543478$; $a_{12} = 0.326084$; $a_{13} = 0.130438$; $T_{F1} =$ 0.23; $\rho = 1.204$ kg m−3, $V = 5.25$ ms−1, $S = 154$ cm2 and C_D =0.6. $0.675 \leq C_L \leq 1.5$.

B = frequency bias constant

R_{TH} = Governer Regulation parameter for thermal unit

R_G = Governer Regulation parameter for Diesel unit,Hz/ p.u MW

R_{HY} = Governer Regulation parameter for Hydro unit,Hz/ p.u MW

$T_{gh=}$ = Governor time constant of hydro unit,s

T_{di} = time constant of diesel unit,s

K_{di} = gain constant of diesel unit.

T_{sg} = Governor time constant of thermal unit.

K_{PS} = power system gain,Hz/ p.u MW

T_{PS} = power system time constant,s

K_r = Steam turbine reheat gain constant

T_r = Steam turbine reheat time constant,s

T_w = nominal starting time of water in penstock, s

T_t = steam turbine time constant of thermal unit,s

T_{rs} = Hydro turbine speed governer reset time,s

T_{rh} = Hydro turbine speed governer transient time droop constant,s

T_{12} = Synchronization coefficient.

K_{w2}, K_{w3} = Gain constants of wind unit.

T_{w1}, T_{w2} = Time constants of wind unit.

ρ = density of air

V = speed

S = Surface area

C_D = lift coefficient

K_{di} = Gain constant of diesel unit.

T_{di} = Time constant of diesel unit.

CONFLICTS OF INTEREST

The authors declare no conflict of interest.

REFERENCES

[1] E. Çam and I. Kocaarslan, "Load frequency control in two area power systems using fuzzy logic controller," *Energy Convers. Manage.*, vol. 46, no. 2, pp. 233–243, Jan. 2005.

[2] J.-Y. Cao and B.-G. Cao, "Design of fractional order controllers based on particle swarm optimization," in *Proc. 1st IEEE Conf. Ind. Electron. Appl.*, May 2006, pp. 1–6, doi: 10.1109/ICIEA.2006.257091.

[3] A. Demiroren and H. L. Zeynelgil, "GA application to optimization of AGC in three-area power system after deregulation," *Int. J. Electr. Power Energy Syst.*, vol. 29, no. 3, pp. 230–240, Mar. 2007.
[4] J. Nanda, S. Mishra, and L. C. Saikia, "Maiden application of bacterial foraging-based optimization technique in multiarea automatic generation control," *IEEE Trans. Power Syst.*, vol. 24, no. 2, pp. 602–609, May 2009, doi: 10.1109/TPWRS.2009.2016588.
[5] H. Golpîra, H. Bevrani, and H. Golpîra, "Application of GA optimization for automatic generation control design in an interconnected power system," *Energy Convers. Manage.*, vol. 52, no. 5, pp. 2247–2255, May 2011.
[6] S. Panda, B. Mohanty, and P. K. Hota, "Hybrid BFOA–PSO algorithm for automatic generation control of linear and nonlinear interconnected power systems," *Appl. Soft Comput.*, vol. 13, no. 12, pp. 4718–4730, 2013.
[7] R. K. Sahu, S. Panda, and U. K. Rout, "DE optimized parallel 2-DOF PID controller for load frequency control of power system with governor deadband nonlinearity," *Int. J. Electr. Power Energy Syst.*, vol. 49, pp. 19–33, Jul. 2013.
[8] B. K. Sahu, S. Pati, and S. Panda, "Hybrid differential evolution particle swarm optimisation optimised fuzzy proportional–integral derivative controller for automatic generation control of interconnected power system," *IET Gener., Transmiss. Distrib.*, vol. 8, no. 11, pp. 1789–1800, 2014, doi: 10.1049/iet-gtd.2014.0097.
[9] J. Nanda, M. Sreedhar, and A. Dasgupta, "A new technique in hydro thermal interconnected automatic generation control system by using minority charge carrier inspired algorithm," *Int. J. Electr. Power Energy Syst.*, vol. 68, pp. 259–268, Jun. 2015.
[10] P. Dash, L. C. Saikia, and N. Sinha, "Flower pollination algorithm optimized PI-PD cascade controller in automatic generation control of a multi-area power system," *Int. J. Electr. Power Energy Syst.*, vol. 82, pp. 19–28, Nov. 2016.
[11] R. K. Sahu, S. Panda, U. K. Rout, and D. K. Sahoo, "Teaching learning based optimization algorithm for automatic generation control of power system using 2-DOF PID controller," *Int. J. Elect. Power Energy Syst.*, vol. 77, no. 1, pp. 287–301, 2016.
[12] A. Saha and L. C. Saikia, "Utilisation of ultra-capacitor in load frequency control under restructured STPP-thermal power systems using WOA optimised PIDN-FOPD controller," *IET Gener., Transmiss. Distrib.*, vol. 11, no. 13, pp. 3318–3331, Sep. 2017, doi: 10.1049/iet-gtd.2017.0083.
[13] D. K. Gupta, R. Naresh, and A. V. Jha, "Automatic generation control for hybrid hydro-thermal system using soft computing techniques," in *Proc. 5th IEEE Uttar Pradesh Sect. Int. Conf. Electr., Electron. Comput. Eng. (UPCON)*, Nov. 2018, pp. 1–6, doi: 10.1109/UPCON.2018.8597013.
[14] M. H. Hany, "Whale optimisation algorithm for automatic generation control of interconnected modern power systems including renewable energy sources," *IET Gener., Transm. Distrib.*, vol. 12, no. 3, pp. 607–614, Feb. 2018.
[15] S. M. Abd-Elazim and E. S. Ali, "Load frequency controller design of a two-area system composing of PV grid and thermal generator via firefly algorithm," *Neural Comput. Appl.*, vol. 30, no. 2, pp. 607–616, Jul. 2018, doi: 10.1007/s00521-016-2668-y.
[16] A. V. Jha, D. K. Gupta, and B. Appasani, "The PI controllers and its optimal tuning for load frequency control (LFC) of hybrid hydro-thermal power systems," in *Proc. Int. Conf. Commun. Electron. Syst. (ICCES)*, Jul. 2019, pp. 1866–1870, doi: 10.1109/ICCES45898.2019.9002150.
[17] Y. Cao, Y. Wu, L. Fu, K. Jermsittiparsert, and N. Razmjooy, "Multi-objective optimization of a PEMFC based CCHP system by meta-heuristics," *Energy Rep.*, vol. 5, pp. 1551–1559, Nov. 2019.
[18] T. K. Mohapatra, A. K. Dey, and B. K. Sahu, "Employment of quasi oppositional SSA-based two-degree-of-freedom fractional order PID controller for AGC of assorted source of generations," *IET Gener., Transmiss. Distrib.*, vol. 14, no. 17, pp. 3365–3376, 2020.
[19] D. K. Gupta, A. K. Soni, A. V. Jha, S. K. Mishra, B. Appasani, A. Srinivasulu, N. Bizon, and P. Thounthong, "Hybrid gravitational–firefly algorithm-based load frequency control for hydrothermal two-area system," *Mathematics*, vol. 9, no. 7, p. 712, 2021, doi: 10.3390/math9070712.
[20] B. Appasani, A. V. Jha, D. K. Gupta, N. Bizon, and A. Srinivasulu, "An improved particle swarm optimization technique and its application in load frequency control," in *Proc. 13th Int. Conf. Electron., Comput. Artif. Intell. (ECAI)*, Jul. 2021, pp. 1–5, doi: 10.1109/ECAI52376.2021.9515171.
[21] D. Wang, F. Chen, B. Meng, X. Hu, and J. Wang, "Event-based secure H_∞ load frequency control for delayed power systems subject to deception attacks," *Appl. Math. Comput.*, vol. 394, Apr. 2021, Art. no. 125788.
[22] L. C. Saikia, S. Mishra, N. Sinha, and J. Nanda, "Automatic generation control of a multi area hydrothermal system using reinforced learning neural network controller," *Int. J. Electr. Power Energy Syst.*, vol. 33, no. 4, pp. 1101–1108, May 2011.
[23] S. Padhy and S. Panda, "A hybrid stochastic fractal search and pattern search technique based cascade PI-PD controller for automatic generation control of multi-source power systems in presence of plug in electric vehicles," *CAAI Trans. Intell. Technol.*, vol. 2, no. 1, pp. 12–25, 2017.
[24] Y. Arya, "Improvement in automatic generation control of two-area electric power systems via a new fuzzy aided optimal PIDN-FOI controller," *ISA Trans.*, vol. 80, pp. 475–490, Sep. 2018.
[25] G. Sharma, A. Panwar, Y. Arya, and M. Kumawat, "Integrating layered recurrent ANN with robust control strategy for diverse operating conditions of AGC of the power system," *IET Gener., Transmiss. Distrib.*, vol. 14, no. 18, pp. 3886–3895, Sep. 2020.
[26] J. R. Nayak, B. Shaw, and B. K. Sahu, "Novel application of optimal fuzzy-adaptive symbiotic organism search-based two-degree-of-freedom fuzzy proportional integral derivative controller for automatic generation control study," *Int. Trans. Elect. Energy Syst.*, vol. 30, no. 5, 2020, Art. no. e12349, doi: 10.1002/2050-7038.
[27] M. Sharma, S. Dhundhara, Y. Arya, and S. Prakash, "Frequency stabilization in deregulated energy system using coordinated operation of fuzzy controller and redox flow battery," *Int. J. Energy Res.*, vol. 45, no. 5, pp. 7457–7475, Apr. 2021.
[28] C. A. Monje, B. M. Vinagre, V. Feliu, and Y. Chen, "Tuning and auto-tuning of fractional order controllers for industry applications," *Control Eng. Pract.*, vol. 16, no. 7, pp. 798–812, Jul. 2008.
[29] S. E. Hamamci, "Stabilization using fractional-order PI and PID controllers," *Nonlinear Dyn.*, vol. 51, nos. 1–2, pp. 329–343, Oct. 2007, doi: 10.1007/s11071-007-9214-5.
[30] J. Nanda, S. Mishra, P. G. Mishra, and K. V. Sajith, "A novel classical controller for automatic generation control in thermal and hydrothermal systems," in *Proc. Joint Int. Conf. Power Electron., Drives Energy Syst. Power India*, Dec. 2010, pp. 1–6, doi: 10.1109/PEDES.2010.5712439.
[31] R. Vilanova, V. M. Alfaro, and O. Arrieta, "Simple robust autotuning rules for 2-DoF PI controllers," *ISA Trans.*, vol. 51, no. 1, pp. 30–41, Jan. 2012.
[32] D. H. Kim, "Design and tuning approach of 3-DOF emotion intelligent PID (3-DOF-PID) controller," in *Proc. 6th UKSim/AMSS Eur. Symp. Comput. Modeling Simulation*, Nov. 2012, pp. 74–77, doi: 10.1109/EMS.2012.93.
[33] S. Debbarma, L. C. Saikia, and N. Sinha, "AGC of a multi-area thermal system under deregulated environment using a non-integer controller," *Electric Power Syst. Res.*, vol. 95, pp. 175–183, Feb. 2013.
[34] Y. Arya, "AGC performance enrichment of multi-source hydrothermal gas power systems using new optimized FOFPID controller and redox flow batteries," *Energy*, vol. 127, pp. 704–715, May 2017.
[35] J. R. Nayaka, B. Shawa, and B. K. Sahu, "Application of adaptive-SOS (ASOS) algorithm based interval type-2 fuzzy-PID controller with derivative filter for automatic generation control of an interconnected power system," *Eng. Sci. Technol., Int. J.*, vol. 21, pp. 465–485, Jun. 2018.
[36] E. Celik, N. Öztürk, Y. Arya, and C. Ocak, "(1+ PD)-PID cascade controller design for performance betterment of load frequency control in diverse electric power systems," *Neural Comput. Appl.*, vol. 33, no. 22, pp. 15433–15456, 2021.
[37] Y. Arya, N. Kumar, P. Dahiya, G. Sharma, E. Çelik, S. Dhundhara, and M. Sharma, "Cascade-I$^{\lambda}$D$^{\mu}$N controller design for AGC of thermal and hydro-thermal power systems integrated with renewable energy sources," *IET Renew. Power Gener.*, vol. 15, no. 3, pp. 504–520, 2021.
[38] Y. Arya, P. Dahiya, E. Çelik, G. Sharma, H. Gözde, and I. Nasiruddin, "AGC performance amelioration in multi-area interconnected thermal and thermal-hydro-gas power systems using a novel controller," *Eng. Sci. Technol., Int. J.*, vol. 24, no. 2, pp. 384–396, Apr. 2021.
[39] R. J. Abraham, D. Das, and A. Patra, "Automatic generation control of an interconnected hydrothermal power system considering superconducting magnetic energy storage," *Int. J. Electr. Power Energy Syst.*, vol. 29, no. 8, pp. 571–579, Oct. 2007.
[40] T. S. Bhatti, "AGC of two area power system interconnected by AC/DC links with diverse sources in each area," *Int. J. Electr. Power Energy Syst.*, vol. 55, pp. 297–304, Feb. 2014.
[41] A. Saha and L. C. Saikia, "Performance analysis of combination of ultra-capacitor and superconducting magnetic energy storage in a thermal-gas AGC system with utilization of whale optimization algorithm optimized cascade controller," *J. Renew. Sustain. Energy*, vol. 10, no. 1, Jan. 2018, Art. no. 014103.

[42] H. Hu, L. Zhang, Y. Bai, P. Wang, and X. Tan, "A hybrid algorithm based on squirrel search algorithm and invasive weed optimization for optimization," *IEEE Access*, vol. 7, pp. 105652–105668, 2019, doi: 10.1109/ACCESS.2019.2932198.
[43] M. Jain, V. Singh, and A. Rani, "A novel nature-inspired algorithm for optimization: Squirrel search algorithm," *Swarm Evol. Comput.*, vol. 44, pp. 148–175, Feb. 2019.

GEETANJALI DEI received the B.E. degree from the Department of Electrical Engineering, University College of Engineering, Burla, Odisha, and the M.Tech. degree in power system engineering from the Veer Surendra Sai University of Technology, Burla, in 2010. She is currently pursuing the Ph.D. degree in automatic generation control (deregulated environment). She is currently working as an Assistant Professor with the Kalinga Institute of Industrial Technology, Odisha. Her research interests include soft computing, power system operation and control, and automatic generation control.

DEEPAK KUMAR GUPTA was born in Lucknow, Uttar Pradesh, India, in 1990. He received the B.Tech. degree in electrical engineering from the Babu Banarasi Das National Institute of Technology and Management, Lucknow, in 2011, the M.Tech. degree in power systems from NIT Hamirpur, in 2013, and the Ph.D. degree from the Indian Institute of Technology (BHU) Varanasi, in 2018. His current research interests include control of power systems, FACTS devices, WAMS, optimization techniques, and renewable energy.

BINOD KUMAR SAHU (Member, IEEE) received the degree in electrical engineering from the Institution of Engineers, India, in 2001, the M.Tech. degree from NIT Warangal, in 2003, and the Ph.D. degree from Siksha 'O' Anusandhan (Deemed to be University), in 2016. He is currently working as an Associate Professor at the Institute of Technical Education and Research (ITER), Siksha 'O' Anusandhan (Deemed to be University). His research interests include automatic generation control, fuzzy logic-based control, soft computing techniques, and time series forecasting. Since 2014, he is a member of IET.

AMITKUMAR V. JHA received the B.E. degree from the University of Pune, India, in 2012, and the M.Tech. degree from IIT Guwahati, India, in 2015. He is currently pursuing the Ph.D. degree with the Kalinga Institute of Industrial Technology (Deemed to be University), India. He has been an Assistant Professor with the School of Electronics Engineering, Kalinga Institute of Industrial Technology, since 2015. He has authored many papers in international conferences and journals. His research interests include computations, communication networks, and smart grids. To his credits, there are two Best Paper Award in IEEE International Conferences held in Japan and Romania.

BHARGAV APPASANI received the Ph.D. degree from the Birla Institute of Technology and Science, in 2018. He is currently working as an Assistant Professor with the School of Electronics Engineering, Kalinga Institute of Industrial Technology, India. He has published over 70 articles in reputed international journals and conferences. He has two patents filed to his credit and has published a book with Springer. He is an Academic Editor of *Journal of Electrical and Computer Engineering* (Hindawi).

HOSSAM M. ZAWBAA was born in Cairo, Egypt, in 1987. He received the B.Sc. and M.Sc. degrees from the Faculty of Computers and Information, Cairo University, Giza, Egypt, in 2008 and 2012, respectively, and the Ph.D. degree from Babeş-Bolyai University, Cluj-Napoca, Romania, in 2018. He is currently an Assistant Professor at the Faculty of Computers and Artificial Intelligence, Beni-Suef University, Beni Suef, Egypt. He has authored or coauthored over 80 research publications in peer-reviewed reputed journals and international conference proceedings. His research interests include computational intelligence, machine learning, computer vision, and natural language understanding. He has been rated as one of the top 2% scientists worldwide by Stanford in the field of AI, in 2020 and 2021. He has been awarded the State Encouragement Award in the field of engineering sciences from the Academy of Scientific Research and Technology, Egypt, in 2020.

SALAH KAMEL received the international Ph.D. degree from Jaen University, Spain (Main), and Aalborg University, Denmark (Host), in January 2014. He is currently an Associate Professor with the Department of Electrical Engineering, Aswan University. He is also the Leader of the Advanced Power Systems Research Laboratory (APSR Lab), Power Systems Research Group, Aswan, Egypt. His research interests include power system analysis and optimization, smart grid, and renewable energy systems.